INORGANIC CHEMISTRY
FRONTIERS

CHINESE CHEMICAL SOCIETY

ROYAL SOCIETY OF CHEMISTRY

REVIEW

View Article Online
View Journal | View Issue

Cite this: *Inorg. Chem. Front.*, 2023, **10**, 7126

The role of niobium in layered oxide cathodes for conventional lithium-ion and solid-state batteries

Barbara Nascimento Nunes, *[a] Wessel van den Bergh,*[a] Florian Strauss,[a] Aleksandr Kondrakov,[a,b] Jürgen Janek [a,c] and Torsten Brezesinski *[a]

Received 14th September 2023,
Accepted 7th November 2023

DOI: 10.1039/d3qi01857a

rsc.li/frontiers-inorganic

Layered transition metal oxides (LTMOs), such as the $LiNi_xCo_yMn_{1-x-y}O_2$ family, are the primary class of cathode active materials (CAMs) commercialized and studied for conventional lithium-ion (LIB) and solid-state battery (SSB) application. Despite nearly three decades of progress in improving stability, capacity, and cost, research has intensified to match global demand for high-performance materials. Nevertheless, (de)lithiation leads to irreversible degradation and subsequent capacity fading due to (chemo)mechanical particle disintegration and (electro)chemical side reactions. In this regard, surface and bulk modifications of CAMs by coating and doping/substitution are common strategies to enhance and support the electrochemical performance. Niobium has been featured in many studies exhibiting its advantages as a bulk dopant, where its ionic radius and unique valence character with respect to the metals used in LTMOs help prevent different degradation phenomena and therefore enhance performance. In addition, several niobium-based oxides ($LiNbO_3$, Li_3NbO_4, Nb_2O_5, *etc.*) have been employed as a coating to increase cycling stability and rate capability through reduced surface degradation. Herein we illustrate how niobium serves as a coating constituent and a dopant, and discuss current understanding of underlying mechanisms, gaps in knowledge, and considerations for its use in a coating and/or as dopant in LTMO cathodes.

1. Introduction

The combination of higher energy density, cycle life, safety, and faster charging, compared to other battery chemistries, has promoted lithium-ion batteries (LIBs) to a widespread power source for a broad range of applications, from portable electronic devices to electric vehicles and stationary energy-storage systems.[1] Since $LiCoO_2$ (LCO) came about as a new cathode active material (CAM) for high energy density batteries

Barbara Nascimento Nunes

Barbara Nascimento Nunes has a chemistry background and completed her cotutelle PhD in 2022, jointly from Leibniz University Hannover and Federal University of Uberlandia. Currently, she is a post-doctoral researcher at BELLA at the Karlsruhe Institute of Technology focusing on the development of cathode materials for lithium-ion batteries.

Wessel van den Bergh

Wessel van den Bergh is a postdoctoral researcher at BELLA at the Karlsruhe Institute of Technology. His research interests are focused on the use of controlled design methodologies to study the relationship between material features and electrochemical behavior for energy-storage applications.

---

[a] *Battery and Electrochemistry Laboratory (BELLA), Institute of Nanotechnology, Karlsruhe Institute of Technology (KIT), Herrmann-von-Helmholtz-Platz 1, 76344 Eggenstein-Leopoldshafen, Germany. E-mail: barbara.nunes@kit.edu, wessel.saarberg@kit.edu, torsten.brezesinski@kit.edu*

[b] *BASF SE, Carl-Bosch-Str. 38, 67056 Ludwigshafen, Germany*

[c] *Institute of Physical Chemistry & Center for Materials Research (ZfM/LaMa), Justus-Liebig-University Giessen, Heinrich-Buff-Ring 17, 35392 Giessen, Germany*

and subsequently the commercialization of LIBs in 1991,[2,3] alternative layered oxides have been explored to improve battery performance and reduce the dependence on cobalt, which has high ethical and economic costs.[4–7] For instance, $LiNiO_2$ (LNO) represents a promising alternative with a local maximum in theoretical specific capacity, however its poor structural stability and low reversible cycling performance limit current commercialization.[8] Other materials, namely the $LiNi_xCo_yMn_{1-x-y}O_2$ (NCM or NMC) and $LiNi_xCo_yAl_{1-x-y}O_2$ (NCA) families, do allow for better cycling stability with the sacrifice of capacity. NCMs have become one of the main classes of CAMs commercialized and studied for LIBs and solid-state batteries (SSBs).[9,10] Due to the global demand for improved batteries in all aspects, there is a general movement to higher nickel content for greater capacity, a transition from flammable liquid electrolyte to solid-electrolyte-based lithium batteries, and evermore material modifications to improve both surface and bulk properties of CAM. Each of these movements in research manifests new challenges, mostly including the need to reduce material degradation and kinetic limitations.

Electrochemical, mechanical, and chemical changes contribute to issues of limited kinetics and stability observed in layered transition metal oxides (LTMOs). Mechanical degradation originates from repeated volume changes in the CAM associated with phase transitions during (de)lithiation that leads to the disintegration of cathode particles and oxygen release from the lattice. This oxygen partially undergoes follow-up reactions with the electrolyte forming CO_2 among other undesired species.[11,12] The most common solution is inclusion of dopants, which can suppress the most mechanically demanding phase transitions ($H2 \rightarrow H3$),[13] or protective surface coatings minimizing gas evolution, for example.[14,15] Chemically, the presence of HF in the commercially common $LiPF_6$-based liquid electrolyte due to trace water results in dissolution of TM species. Here, sacrificial compounds or coatings are introduced to NCM cathodes as a strategy for mitigating this issue. As an electrochemical degradation mechanism, there is the decomposition of electrolyte, leading to the formation of a resistive surface layer (cathode electrolyte interphase, CEI), as well as the phenomenon of degradation of bulk NCM layered structure.[16,17] To address these concerns, specific solutions involving coatings and dopants are implemented in the quest to develop improved battery materials. Coatings, which serve as a controlled, stable CEI, ideally need to offer high ionic conductivity, good chemical resistance, and a simple synthesis process.[18,19] With respect to doping strategies, dopants can modify either a portion of the subsurface or the entirety of the bulk. Regardless of the depth of incorporation, a dopant ideally serves to stabilize the structure of the CAM, such as forming stronger metal–oxygen (M–O) bonds, to reduce oxygen release or increase lithium diffusivity.

Selection of elements and/or compounds to serve as dopants and/or coatings is an on-going process, where the untrained eye may feel that the field is collectively sifting through the periodic table. Regardless of the breadth of exploration for the next best coating or dopant, there have been reports of promising candidates for mainstream implementation. Niobium has been featured in many studies exhibiting its advantages as an elemental dopant and of its various oxide phases ($LiNbO_3$, Li_3NbO_4, Nb_2O_5, *etc.*) as coating agents. Overall, its common and most stable oxidation state of Nb^{5+} shows high affinity to oxygen and forms thermally and chemically stable oxides.[20] In addition, it has a comparable ionic radius of 0.64 Å, yet distinct valence character, with respect to the common metal species used in LTMOs, *e.g.*, Ni^{3+} (0.56 Å), Ni^{2+} (0.69 Å), Co^{3+} (0.55 Å), Mn^{3+} (0.58 Å), Al^{3+} (0.54 Å), and Li^{+} (0.76 Å).[21] These characteristics translate to an observed reduction in degradation and improvements to lithium diffusion kinetics when Nb^{5+} is employed as a dopant. Other element dopants with comparable ionic radius and higher valence than the TMs in LTMOs, such as V^{5+},[22–24] Ta^{5+},[25–27] Mo^{6+},[28–30] and W^{6+},[31–33] have also been reported to exhibit similar improvements. Another work has outlined the impact of these and various other dopants and coating materials on Ni-rich CAMs.[34] Experimentally, many niobium precursors are reported in the literature for use in both doping and coating approaches. A crucial point to consider is that the specific niobium location in lithium-based LTMOs depends on

Florian Strauss

Florian Strauss received his PhD in 2016, under the supervision of Prof. Tarascon (Collège de France, Paris) and Prof. Dominko (National Institute of Chemistry, Ljubljana). He spent several years as a post-doctoral researcher at BELLA at the Karlsruhe Institute of Technology and is currently a junior group leader at the Institute of Nanotechnology exploring novel electrolytes for solid-state batteries.

Aleksandr Kondrakov

Aleksandr Kondrakov received his diploma in Chemistry from the Lomonosov Moscow State University in 2010 and a PhD in Chemistry from the Karlsruhe Institute of Technology in 2014. After postdoctoral years spent at BELLA, he joined BASF Battery Materials in 2017 working on the development of layered Ni-rich oxide cathode materials. As a lab team leader of BELLA, he focuses on the research of next-generation battery materials.

several factors, including the niobium precursor concentration, the synthesis conditions (especially temperature), and the crystal structure of CAM. Recently, Xin *et al.* reported that the retention of niobium on the $LiNi_{0.8}Co_{0.1}Mn_{0.1}O_2$ (NCM811) surface or its diffusion into the bulk depends on the treatment temperature.[35] Through different characterization techniques, evidence was found that the NCM is coated with niobium at lower temperatures (400 and 500 °C), whereas Nb-doping (incorporation) occurs at higher temperatures (600, 700, and 800 °C). In this case, the presence of niobium in two different forms, coating and substitution, offers distinct benefits. The Nb-based coating formed $LiNbO_3/Li_3NbO_4$ phases, which provide surface stabilization, decrease the first-cycle loss, and enhance rate capability. Concurrently, niobium substitution improves the capacity retention on extended cycling by stabilizing the lattice.[35]

Furthermore, $LiNbO_3$ is widely recognized as a coating material for LIBs and SSBs, demonstrating strong performance compared to other reported coatings. As a crystalline material, it shows a very low ionic conductivity ($\sim 10^{-18}$ S cm^{-1}), however if amorphous, its conductivity is increased by several orders of magnitude, making it suitable as an ionically conducting coating material.[36–39] Moreover, $LiNbO_3$ possesses a high (electro)chemical stability, a necessary feature for CAM coatings.[40–42] Therefore, there are numerous studies in the literature reporting the positive effects of niobium as a dopant or coating constituent for LTMOs. However, to the best of the authors' knowledge, there is no report that compiles and analyzes all of these mentioned aspects. This review will illustrate how niobium serves as a coating and dopant, highlight the current understanding of the underlying mechanisms, and discuss gaps in knowledge and considerations for its use in LTMO cathodes.

2. Coating

Coatings can first and foremost be considered as an artificial protective layer between active material and electrolyte. With respect to cathodes, as is the focus of this review, a passivation layer (interphase) begins to form when three conditions are met: the electrolyte and active material are in contact, the HOMO of species in the electrolyte is greater in energy than the LUMO of the cathode, and ionic transfer is possible. When all these conditions are met, then this leads to oxidation of the electrolyte. However, one should note that interphase formation is a complex process and the subject of focused study, where the description above can be seen as a qualitative view of the phenomena. These oxidized species decompose on the surface of the cathode and form the CEI and gaseous side products (*e.g.*, CO_2 and POF_3).[13,43] The CEI acts as a kinetically stable interface, which prevents further electrolyte decomposition, as it is ionically permeable yet electronically insulating.[44,45] However, the CEI's organic and inorganic components can further be (electro)chemically decomposed. This process can lead to dissolution/removal and subsequent reformation of the CEI by consuming "fresh" electrolyte and continuous gas evolution. In addition to containing soluble species, repeated cycling and subsequent volumetric changes cause cracks in the surface of both the active material particle and CEI, which in turn results in further consumption of electrolyte and growth of the CEI. Furthermore, commercial liquid electrolytes use $LiPF_6$ as their conducting salt, which, when in the presence of residual moisture, reacts to form HF (eqn (1) and (2)), which will dissolve susceptible metal species.[46]

$$LiPF_{6(dissolved)} + H_2O \leftrightarrow LiF_{(s)} + 2HF_{(dissolved)} + POF_{3(dissolved)} \tag{1}$$

$$PF_{5(dissolved)} + H_2O \leftrightarrow 2HF_{(dissolved)} + POF_{3(dissolved)} \tag{2}$$

However, even if the CEI is absolutely stable, theoretical models suggest that the ionic conductivity is low at 10^{-15}–10^{-17} S cm^{-1},[47–49] which can result in lithium diffusivity limitations. Low conductivity and a continuously growing CEI lead to large overpotentials that limit energy efficiency and reduce the capacity.[50] While one can make modifications to the electrolyte through the use of different salts, solvents, and additives, they risk being oxidized to also form CEI when reaching sufficiently high voltage. The alternative is producing a predesigned CEI (coating) that will have a controlled thickness, reactivity, and diffusivity. Coatings serve multiple purposes,

Jürgen Janek

Jürgen Janek holds a chair for Physical Chemistry at the Justus-Liebig-University Giessen and is one of the scientific directors of BELLA. He received his doctoral degree in Physical Chemistry and was a visiting professor at Seoul National University, Tohoku University, and Université d'Aix-Marseille. Current key interests include solid-state batteries, solid electrolytes, and kinetics at interfaces.

Torsten Brezesinski

Torsten Brezesinski is a chemist by training, earning his doctorate in Physical Chemistry from the MPI of Colloids and Interfaces/University of Potsdam in 2005. He is laboratory manager of BELLA and group leader at the Institute of Nanotechnology. His work encompasses, among others, the characterization of battery materials for electrochemical energy storage.

which benefit the performance and stability of the CAM. First, coatings serve as a physical barrier between CAM and electrolyte, which mitigates the formation of (excess) CEI as well as side reactions, such as metal dissolution, electrolyte consumption, and gas formation. Second, designed coatings ideally have a greater permittivity (1/resistance) than "native" CEIs, thereby minimizing the overpotential that may otherwise intensify side reactions and lead to reduced capacity. Similar benefits are observed in SSBs, where (electro)chemical solid electrolyte decomposition and related performance decay are prevented.[51,52] Lastly, experimental data suggest that coatings can increase the temperature at which cathodes experience thermal runaway, which is critical for commercial liquid-electrolyte-based LIBs.[35,53–56]

Despite a plethora of compositional options for coatings, Nb-based ones represent a promising method to stabilize cathode/electrolyte interfaces. $LiNbO_3$ can be considered the quintessential Nb-based coating and can be prepared in multiple ways, including sol–gel,[42,53,57–73] dry coating,[55,61,74–79] and atomic layer deposition (ALD).[80,81] Sol–gel derived coatings require the least demand with regards to equipment, and the procedure is mature. Typically, CAM particles are suspended in a solvent together with Nb-alkoxides or chlorides and an extra source of lithium (usually lithium ethoxide) is included. This process can take place in alcohols, which are subsequently evaporated to yield a gel. *Via* changing the precursor ratios and adding a lithium source, different Nb-oxide-based compositions, such as Nb_2O_5, $LiNbO_3$, and Li_3NbO_4, can be targeted. This mixture is then calcined (usually in air or oxygen) at different temperatures, which determines whether niobium remains at the surface or migrates into the bulk of the CAM.[56] However, sol–gel derived coatings are observed to suffer from non-uniformity, although they can be rapidly prepared through a simple process. Moreover, it has been recently recognized that coatings prepared *via* the sol–gel method always contain (amorphous) lithium carbonate, which appears to have a significant impact on the resulting performance of the CAM, especially in SSBs.[67,73,82–84] Dry coating is an alternative procedure, where preformed (preferably nanocrystalline) $LiNbO_3$ is mixed with CAM powder under moderate or high energy conditions (milling). The mixture is then calcined to sinter the coating and the CAM together. While requiring specialized yet simple equipment, the use of cheaper starting materials is attractive, even if coating uniformity is still non-ideal. To yield a conformal coating on CAM particles, ALD is the method of choice, however at the expense of costly equipment.

Regardless of the technique, Nb-based oxides exhibit stability against aggressive acid conditions. For instance, a clear illustration of this resilience is observed on sample preparation protocols for inductively coupled plasma (ICP) optical emission spectroscopy (OES), where concentrated acids at high temperatures are required to achieve niobium dissolution.[85,86] It should be noted that alternatively employing a protective coating as a sacrificial HF scavenger might not be an optimal design choice. Furthermore, scavengers with extensive surface areas (nanoparticles) can be introduced as additives rather than implementing a more complex coating process. Regardless, it is clear that Nb-based coatings do reduce metal dissolution, where they most likely act as a physical barrier preventing TM ion migration to the electrolyte.[76]

To understand composition–morphology related properties of nanoscale coatings, a thorough characterization down to the atomic scale is needed. Initially, scanning electron microscopy (SEM) is often performed to confirm that the particle morphology is not affected during the coating formation. For instance, Fig. 1a–f shows images of Nb_2O_5-coated NCM622 in comparison to the pristine material, where the presence of Nb_2O_5 did not alter the overall morphology or average particle size of CAM.[76] While there may be slight textural differences at the surface,[70,72] additional analytical techniques are needed to characterize the morphology and composition of the coating. Coatings prepared *via* sol–gel methods tend to show a partial agglomeration on the CAM surface.[70,72] It should be noted that several studies explicitly mention the thickness. The optimal thickness can generally vary within the range of ~2 to 10 nm.[42,56,58,60,62,65,67,68,79–81,87–89] Nevertheless, only one of them quantifies the degree of uniformity or variation in thickness. This particular study employed atomic force microscopy (AFM) to measure particle roughness, which decreased with added coating, likely suggesting a reduction in initial porosity.[81] This is in the context of reports that vary coating thickness by molar or weight percentage and observe differences in performance. In general, both extremely thin and thick coatings come with limitations. Very thin coatings fail to fully cover particles, while thick coatings hinder charge transfer, sacrificing rate capability and reducing specific capacity due to increased resistance.[58,80,87,88] Therefore, considering that physical thickness of the coating rather than molar or weight fraction with respect to the CAM will dictate performance, we recommend examining thickness as being more relevant. To do so, thin sample specimens prepared by focused ion beam (FIB) milling/slicing are required. This allows for an examination of the

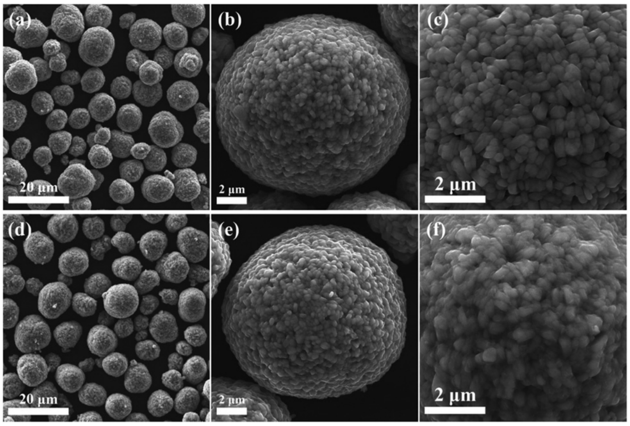

Fig. 1 (a–c) SEM images of a pristine $LiNi_{0.6}Co_{0.2}Mn_{0.2}O_2$ (NCM622) sample. (d–f) SEM images of coated NCM622 prepared from a ball-milling method with Nb_2O_5 (0.5 mol%). Reproduced with permission from ref. 76. Copyright 2021, Elsevier.

coating *via* energy dispersive X-ray spectroscopy (EDS) line scans[64,87] (see Fig. 2a and b) and transmission electron microscopy (TEM),[64,80,87] which is however spatially limited to a small range of the surface layer. Interestingly, X-ray photoelectron spectroscopy (XPS) analysis reveals that the distribution of coating ions can strongly depend upon the choice of coating method. XP spectra were obtained by gradually removing surface layers through ion etching.[87] A thicker layer formed when using a coating methodology of introducing niobium, while including niobium with the precursor reagents before CAM synthesis led to ion migration into the bulk structure.

Additionally, due to the proclivity of niobium to diffuse into the bulk lattice, it stands out that few works examined the gradient of niobium concentration from the surface to the core.[35,60,65,87,90] With the advent of studies beginning to understand the implications of gradient-doped NCM CAMs, this is a feature that should be studied in detail when observed. X-ray diffraction (XRD) analysis serves to see the effect of niobium in the bulk, whose introduction usually affects the lattice parameters.[79] The effect of niobium as a bulk dopant is discussed in the doping section below. XRD also shows evidence that procedures that originally target Nb_2O_5 coatings may convert it to $LiNbO_3$,[77,79] even in the absence of an additional lithium source.[56] One can verify the formation of a specific coating with X-ray absorption spectroscopy (XAS), even when the coating is below the limit of detection for XRD. Fig. 3 displays peaks associated with transitions from the 2p orbital of niobium in different reference materials. In this particular case, peak shift analysis provided insight into the chemical state of the coating.[57] In the absence of a deliberate external source, it is probable that residual lithium on the CAM's surface or lithium from within the bulk serves as the source for $LiNbO_3$ formation. This may lead to the unintended increase of Li^+/Ni^{2+} cation mixing (antisite defects, $\text{Ni}_{\text{Li}}^{\bullet}$) that degrades the performance of the CAM, as discussed below.

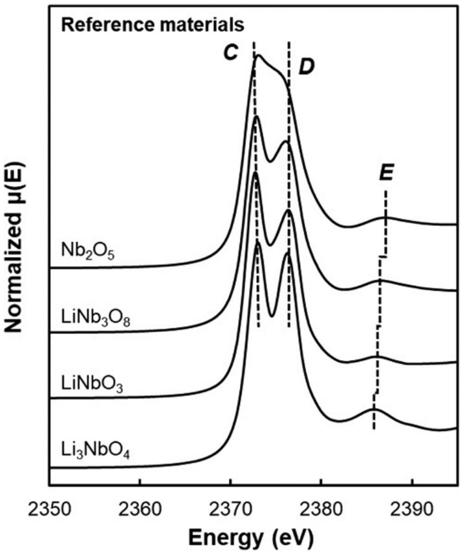

Fig. 3 XAS of the Nb L_3-edge of reference materials with Nb^{5+} oxidation state. Dotted lines C and D correspond to $LiNbO_3$ peak position, while dotted line E is peak position of each reference material. Reproduced with permission from ref. 57. Copyright 2023, American Chemical Society.

Crystalline $LiNbO_3$ can be detected through XRD analysis. However, employing XRD for characterizing nanoscale coatings is often impractical due to the limited sensitivity of most in-house instruments.[87,91,92] Any observation of reflections from coatings likely comes from agglomerated species or coatings that exceed practical thickness, as shown in Fig. 4, in which at 20 wt% loading, agglomeration and layering is large

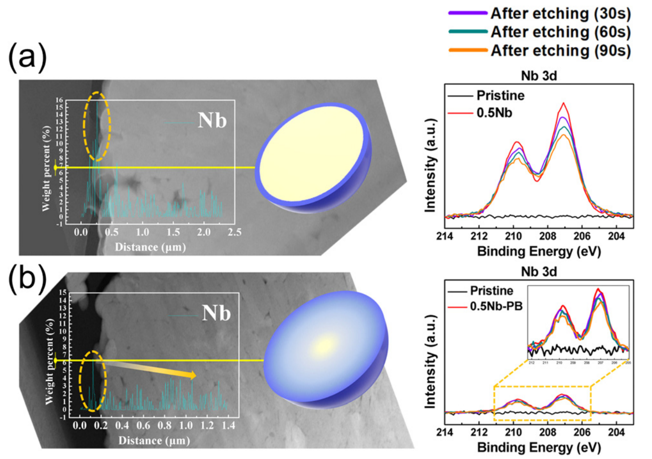

Fig. 2 Cross-sectional scanning TEM (STEM) with EDS line profiles of Nb across the yellow line for $LiNi_{0.82}Co_{0.12}Mn_{0.06}O_2$. Shown to the right is the corresponding material's Nb 3d XP spectra with different etch times. Panel (a) refers to a coating methodology of introducing Nb, while panel (b) refers to a route of including Nb with the precursor reagents. Adapted from ref. 87. Copyright 2021, American Chemical Society.

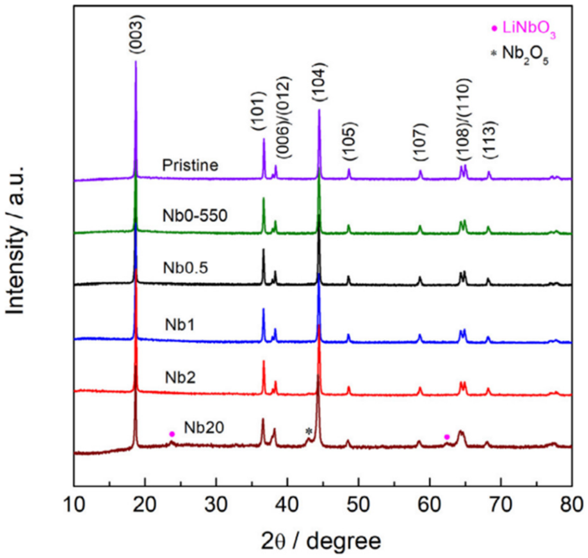

Fig. 4 XRD patterns of NCM622 coated with different loadings (wt%) of $LiNbO_3$ prepared from an ammonium niobium oxalate sol–gel method. Reproduced with permission from ref. 56. Copyright 2021, Elsevier.

enough to show Nb-based reflections.[56,58,75] XRD signals linked to the coating are evident in several sol–gel-based approaches[56,58,59,70,93] in contrast to ALD-based reports.[87]

XPS is commonly used to characterize the composition and state of the LTMO surface, however, frequently, extrapolations are made that require careful consideration. Firstly, XPS (Nb 3d) can detect the oxidation state of the niobium,[53,56,94] which is usually observed to be +5 and can reflect either $LiNbO_3$ or Nb_2O_5. This can be applied to other atomic species; works reporting Nb_2O_5 coatings performed XPS (Ni 2p) to note an increase in Ni^{2+} species at the surface,[76,79] likely due to the $LiNbO_3$ formation (resulting in extraction of lithium from the bulk of the CAM). Simultaneously, some ions diffuse into the bulk, and the high valence state of niobium lowers the nickel oxidation state to Ni^{2+}, thereby driving it into the lithium layer.[60,77] $LiNbO_3$ does not affect the Ni^{2+} fraction at milder temperatures (*e.g.*, ≤550 °C).[42,69] In contrast to these observations, other work describes that niobium coating actually reduces near-surface Ni^{2+},[78] which could also be expected for a surface-stabilizing coating. The authors also show XRD Rietveld refinements of their LTMO and coated material, indicating a lower fraction of $Ni_{Li}^{\bullet}$ defects, however often do so with suspiciously low R_{wp} values for lab-scale diffractometers.[64,95] As will be discussed later, complementary techniques to determine the effect of niobium on point defects should be employed to build a stronger case. Secondly, XPS can indicate the migration of niobium from the surface to the bulk through loss of intensity of the corresponding spectra, which correlates with increasing preparation temperature.[35] When looking at other XPS peaks, it is observed that Nb-based coatings reduce the fraction of Li_2CO_3,[35] a surface carbonate that relates to decomposed electrolyte,[55] air exposure,[83,96] and insulating LiF. Degradation of the surface can be observed with XPS[58] and can be correlated with electrochemical measurements of average surface resistance, charge-transfer resistance, and their rate of growth in LIBs and SSBs.[93]

Turning to performance itself, a meta-analysis of both LIBs and SSBs with $LiNbO_3$-coated NCM CAMs reveals generalizable trends and indicators of its true utility. Fig. 5 is a box-and-whisker plot of a meta-analysis of coated NCMs. Comparisons of relative performance changes were made between the self-described best coating reported and their baseline NCM material; a method that removes the case-by-case comparison and the many minor differences in methodology and testing. Furthermore, unless otherwise demonstrated in the work with certainty, all coatings are assumed to be $LiNbO_3$, despite claims of Nb_2O_5, due to their lack of support evidence to the case. Lastly as a note, due to the variation in number of cycles reported across works, a standard of 100 cycles was selected. For cases, where this information was not explicitly provided, an estimate was calculated based on reported cycling stability and assuming a linear trend of degradation for all materials. This estimation methodology is the case for both the data presented for coatings as well as dopants shown in a later section. Starting with LIB samples, Fig. 5 shows that the introduction of $LiNbO_3$ as a coating had an insignificant effect on the initial discharge capacity (median = 3.3%) while being able to significantly improve cycle retention (median = 12%) and capacity at 1C rate (median = 8.0%). This likely reflects the reduction in surface decomposition and therefore reduced resistance of the material. Regarding SSBs, there is an increase in all metrics, first-cycle capacity (median = 18%), cycle stability (median = 10%), and capacity at 1C rate (median = 28%). While not surprising that there are improvements, it is important to note that the relative increases in rate capability and first-cycle capacity are greater for SSBs than LIBs. This is most likely due to the formation of a much more insulating interface (decomposition) layer in SSBs when using uncoated CAM as compared to LIBs. Regardless of the electrolyte, ionic conductivity of amorphous $LiNbO_3$ is significantly higher than of base NCM. This reflects an average observed relative increase in diffusivity of $LiNbO_3$-coated NCMs by 120% ± 150% (mean ± std. dev., n = 6) and 74% ± 53% (mean ± std. dev., n = 3) for LIBs and SSBs, respectively.[42,56,58,74,76,77,79,81,87,97]

Despite being a point parroted in introductions as critical to improving LIBs, thermal stability, *i.e.*, onset temperature of

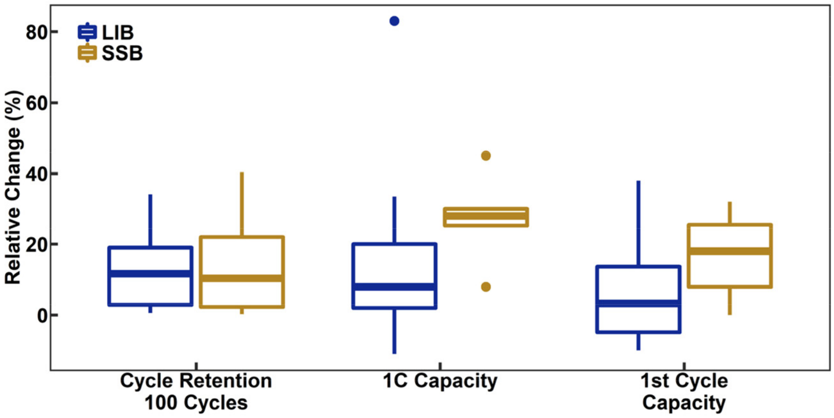

Fig. 5 Box-and-whisker plot of the relative change of capacity retention after 100 cycles, 1C capacity, and first-cycle capacity of $LiNbO_3$ coatings with respect to "bare" NCM CAMs for both LIB and SSB systems. For cycle retention, n = 19 and 9 for LIB and SSB, respectively. For 1C capacity, n = 17 and 6 for LIB and SSB, respectively. For first-cycle capacity, n = 18 and 11 for LIB and SSB, respectively.

exothermic decomposition of a charged CAM, is a factor examined by only two studies, where Nb-based coatings did increase thermal stability by a modest ~4–5%.[35,56] While small in magnitude, it is a self-described "critical" metric that should be examined when modifications are made to NCMs. Because of increased thermal and mechanical stabilities, the application of Nb-based coatings can result in better CAM performance at elevated temperatures both in LIBs[53,56,60,76] and SSBs.[72,73,80,89] $LiNbO_3$ coating offers superior cyclability of chlorine-rich argyrodite-based SSBs using $LiNi_{0.7}Co_{0.1}Mn_{0.2}O_2$ (NCM712) cathodes at different temperatures (−20, 25, and 60 °C).[89] The improved performance at all tested temperatures is attributed to reduced interfacial resistance, as observed by electrochemical impedance spectroscopy (EIS), and structural enhancements, supported by TEM imaging data collected after cycling. Clearly, Nb-based coatings have a positive effect on CAM structure and morphology. While pristine CAMs typically exhibit signs of severe damage, Nb-coated counterparts are often capable of maintaining their initial morphology during cycling, indicating enhanced mechanical stability and leading to reduced exposure of fresh (reactive) surfaces.[42,53,58,60,76,80] Accordingly, XPS analysis provides evidence of partially suppressed side reactions and CEI growth, as seen by less intense peaks of carbon–oxygen, $Li_xPO_yF_z/Li_xPF_y$, and LiF species for LIBs[58,60,93] and oxygenated sulfur and phosphorus species for SSBs.[81,89] In addition, XRD analysis of cycled materials reveals smaller peak shifts and larger intensities for coated CAMs in comparison to their base materials, suggesting that the coating can also effectively alleviate volume variations.[53,79,89] Regardless, these improvements lack greater context, as there is a serious lack of meaningful comparisons or meta-analyses between different coatings and surface species. However, there is a report of comparative performance for coated $Li_{1.2}Mn_{0.54}Ni_{0.13}Co_{0.13}O_2$ cathodes.[75] Nb-based coatings have a high material cost, thus a definitive, cost-effective alternative should be presented if possible, with direct comparison between candidates to decide the best material for large-scale application.

Table 1 is a limited comparison of reported ionic conductivities of common coatings and surface species. While Li_2ZrO_3 may exhibit greater ionic conductivity, this does not directly translate to a better coating material; experimental comparisons or meta-analyses should be done to support such a claim. Other "hybrid" ($Li_aM_bNb_cO_d$; *e.g.*, M = Ti) and Li_3NbO_4 coatings have been tested,[60] however only one direct comparison between these and "standard" Nb-based coatings has been reported to our knowledge.[93] Li_3NbO_4 can be seen as a "non-standard" coating by virtue of the scarcity of reports. It is a compound that is observed to form at higher temperatures, but has not demonstrated greater performance than the more facile to synthesize $LiNbO_3$.[93] Comparable performance to $LiNbO_3$ also reflects observations made for "hybrid" Nb-coatings, *e.g.*, $TiNb_2O_7$.[60] Therefore, unless otherwise demonstrated by future reports, $LiNbO_3$ represents the best option due to its relatively easy of synthesis and good performance.

Table 1 Average Li-ion conductivities of compounds found or added to the surface of NCM CAMs

Coating	Ionic conductivity/S cm^{-1}	Ref.
Amorphous $LiNbO_3$	8.4×10^{-7} (293 K)	98
Li_3PO_4	$\sim 10^{-8}$ (573 K)	99
Li_2CO_3	Ionically insulating (338 K)	100
LiF	$\sim 10^{-14}$ (293 K)	101
Al_2O_3	Ionically insulating (293 K)	102
Crystalline Li_2ZrO_3	8×10^{-5} (293 K)	103

3. Doping

While coatings do address surface-related degradation processes for LTMOs, dopants are mainly implemented to improve structural integrity *via* mitigating irreversible phase transitions during cycling. In addition, better rate capability is also likely achieved because of enhanced electronic and/or ionic conductivity, due to the expansion of lithium diffusion channels and the formation of defects, leading to a reduction in polarization resistance.[104] In some cases, dopants in LTMOs with a high nickel content can result in increased ionic conductivity also by reducing the concentration of unintended defects (*e.g.*, $Ni_{Li}^{\bullet}$) and suppress oxygen release with greater M–O bonding energies.[34,105] From this perspective, high-valence ions are typically employed to improve the stability of Ni-rich LTMO cathodes.[106,107] Mostly, high-valence dopants reside in the TM sites, and consequently increase repulsive force between interlayers.[23,108–110] Compared to Ni^{3+}, Mn^{4+} and Co^{3+} ions (0.53–0.56 Å), they are generally larger and often increase the lithium layer spacing and lattice parameters and therefore lithium diffusivity. Additionally, these ions provide strong M–O bonds and increase the stability of layered structure during the (de)lithiation process. Bond energies of M–O can be found in the literature, some examples are 667 kJ mol^{-1} for Ti–O, 637 kJ mol^{-1} for V–O, and 720 kJ mol^{-1} for W–O, which are higher than that for Ni–O (366 kJ mol^{-1}), Co–O (397 kJ mol^{-1}), Mn–O (362 kJ mol^{-1}), and Al–O (502 kJ mol^{-1}).[21,111] Considering this, Nb^{5+} is a TM dopant that introduces a strong Nb–O bond (727 kJ mol^{-1}),[111] a large but comparable ionic radius of 0.64 Å, and a high valence state.[112] These characteristics ultimately result in significant improvements in material stability and behavior.

It is important to emphasize that the preparation method employed for doped materials can significantly affect the final product. In relation to Nb-doped LTMOs, they are frequently prepared by blending a precursor CAM (pCAM) with proper niobium and lithium sources, followed by subjecting the mixture to the same heating treatment as the base material, which can also vary in temperature and time. Nb_2O_5 is the predominant precursor, followed by niobium oxalates (see Table 2). In this sense, excessive doping can reach a "solubility limit" and migrate to the surface, forming a protective layer that inhibits detrimental side reactions; conversely, a coating can facilitate doping of near-surface regions through diffusion at elevated or sustained calcination temperatures. In such

Table 2 Summary of main electrochemical performances from the literature of Nb-doped LTMOs for LIBs, their respective base material, as well as Nb source and its amount (SC = single crystal, DC = specific discharge capacity, CR = capacity retention after the respective number of cycles)

CAM	Nb source	Amount	1st DC (base)/mA h g^{-1}	CR (base)/%	Cycles	Voltage/V *vs.* Li^+/Li	Ref.
LNO	$H_5Nb_3O_{10}$	1.0 mol%	188.1 (215.9) at 0.1C	91.4 (69.2) at 0.5C	100	2.7–4.3	112
LNO	$C_4H_4NNbO_9$	1.0 mol%	214.1 (233.7) at 0.1C	85.8 (60.1) at 0.5C	200	3.0–4.3	128
$LiNi_{0.925}Co_{0.03}Mn_{0.045}O_2$	Nb_2O_5	0.4 mol%	222.7 (219.5) at 0.1C	77.7 (66.3) at 1C	150	2.8–4.3	132
NCM851005	Nb_2O_3	0.3 mol%	210 (210) at 0.1C	97.0 (80.0) at 1C	100	3.0–4.3	152
NCM831106	Nb_2O_5	1.0 mol%	195 (201.8) at 0.1C	86.6 (61.2) at 1C	200	2.8–4.3	120
NCM831106	$C_4H_4NNbO_9$	1.0 mol%	211.8 (195.5) at 0.2C	86.6 (62.6) at 1C	100	2.7–4.4	118
NCM831205 (SC)	Nb_2O_5	1.0 mol%	198.6 (196.8) at 0.1C	92.7 (72.4) at 1C	150	2.7–4.3	129
$LiNi_{0.8}Co_{0.2}O_2$	Nb_2O_5	1.0 mol%	190.7 (176.6) at 0.2C	90.0 (58.0) at 5C	100	3.0–4.3	136
$LiNi_{0.8}Co_{0.15}Al_{0.05}O_2$	Nb_2O_5	5.0 mol%	192.0 (202.7) at 0.5C	94.2 (69.5) at 0.5C	100	2.8–4.5	133
NMC811	$Nb(HC_2O_4)_5$	1.0 mol%	219.6 (203.3) at 0.2C	92.7 (85.3) at 0.2C	100	2.8–4.6	134
NCM811	Nb_2O_5	1.0 mol%	226.3 (213.2) at 0.05C	94.6 (57.6) at 1C	100	2.7–4.3	104
NCM811	Nb_2O_5	0.5 mol%	189.2 (184.9) at 0.1C	91.9 (79.8) at 1C	300	2.75–4.3	119
NCM811	Nb_2O_5	1.0 wt%	202.8 (163.5) at 2C	81 (55) at 2C	200	2.7–4.5	121
NCM811 (SC)	Nb_2O_5	0.5 mol%	226 (202.5) at 0.1C	92.5 (84.3) at 1C	100	2.7–4.3	122
NCM811	Nb_2O_5	1.0 wt%	200.2 (202.3) at 0.1C	90.6 (82.1) at 0.1C	100	3.0–4.3	130
NCM811 (SC)	$LiNbO_3$	1.0 mol%	209 (199.2) at 0.2C	91.4 (82.3) at 5C	100	2.7–4.6	123
$LiNi_{0.7}Mn_{0.3}O_2$	Nb_2O_5	2.0 mol%	184.3 (185.3) at 0.1C	91.8 (75.8) at 0.2C	50	2.75–4.35	116
NCM712 (SC)	Nb_2O_5	0.05 mol%	204 (200) at 0.1C	85.5 (70.6) at 1C	150	3.0–4.5	145
NCM622	Nb_2O_5	1.0 mol%	188.4 (195.7) at 0.2C	91 (78) at 1C	100	3.0–4.5	78
NCM523	Nb_2O_5	1.0 mol%	159.5 (152.5) at 0.1C	78.7 (73.2) at 0.5C	50	2.5–4.3	131
$Li_{1.2}Mn_{0.53}Ni_{0.27}O_2$	$Nb(HC_2O_4)_5$	1.6 mol%	248.3 (243.5) at 0.1C	85.5 (57.5) at 1C	200	2.0–4.7	124
$Li[Li_{0.2}Ni_{0.2}Mn_{0.6}]O_2$	Nb_2O_5	4.0 mol%	254 (221) at 0.1C	92.3 (83.4) at 0.1C	100	2.0–4.8	117
$Li_{1.2}Mn_{0.54}Ni_{0.13}Co_{0.13}O_2$	$Nb(HC_2O_4)_5$	2.0 mol%	265.8 (236.3) at 0.2C	86.9 (78.3) at 0.2C	100	2.0–4.8	141
$Li_{1.2}Mn_{0.54}Ni_{0.13}Co_{0.13}O_2$	$Nb(C_2H_5O)_5$	3.0 mol%	320 (276) at 0.1C	95 (76) at 0.1C	100	2.0–4.8	137
$Li_{1.2}Mn_{0.54}Ni_{0.13}Co_{0.13}O_2$	Nb_2O_5	2.0 mol%	282.6 (265.8) at 0.05C	87.8 (58.5) at 1C	100	2.5–4.6	142

scenarios, the enhanced electrochemical performance can be attributed to the combined effects of doping and coating.[113] Tungsten is a classic example, which almost exclusively migrates to the surface and forms $Li_xW_yO_z$.[114] Indeed, high-valence elements, such as Nb^{5+}, Ta^{5+}, W^{6+}, and Mo^{6+}, are more likely to have only limited solubility within the crystal structure of Ni-rich CAMs. Specifically, they tend to segregate at the grain boundaries, thereby also suppressing the coarsening of primary particles.[107,115] This poses an interesting design feature, where known solubility limits can be targeted to create both a bulk and surface modification with a single synthesis procedure. The differentiation between doping and coating can often be ambiguous. In fact, annealing conditions seem to play a pivotal role in material modification. Xin *et al.* reported investigations in this regard, where Nb-based coating and substitution were both observed in Ni-rich CAMs depending on temperature conditions.[35,59,65,90] Firstly, NCM811 was modified by the hydrolysis process of lithium and niobium ethoxides, a very typical procedure for CAM coatings. With the 500 °C annealing, some Nb^{5+} ions were observed to penetrate into the parent material and their concentration maintained around 0.2 at% for a few hundred nanometers. Accordingly, there was a decrease in first-cycle capacity loss, alongside enhancements in rate capability and capacity retention, for half-cells tested in the potential window of 2.8–4.6 V.[65] Further studies of synchrotron diffraction showed that $LiNbO_3$ and Li_3NbO_4 phases were initially formed on the CAM surface, and higher temperature treatments (>690 °C) provoked $LiNbO_3$ decomposition and Nb/TM interdiffusion. In this case, Nb^{5+} penetrated into the bulk, resulting consequently in lattice expansion and cation disordering.[35,90] Neutron powder diffraction (NPD) analysis suggested higher Ni^{2+} fraction in NCM and interestingly, a manganese replacement in niobium sites of Li_3NbO_4.[35] Similarly, several works of Nb-doping of LTMOs also mention the presence of new phases of niobium compounds, particularly when high amounts of dopant are used. The main observed phases in XRD patterns are Li_3NbO_4,[116–118] $LiNbO_3$,[78,104,119] and Nb_2O_5,[117] which in general indicates that a solid solution limit was reached and remaining Nb^{5+} ions reacted with the available lithium source, as mentioned before for coated CAMs. Therefore, the probable minimal concentration and widespread distribution of these phases in Nb-modified materials hinder their detection with XRD analysis. Nevertheless, either the effect of these new phases is not further considered or the doped materials with higher amount of niobium are not explored due to their low electrochemical performances. In this sense, it is common to encounter a lack of clarity regarding a possible additional coating in Nb-doped CAMs. This is often associated with the use of limited characterization techniques, which may not offer a complete understanding of the modified material. Another source of uncertainty stems from the doping depth, whether Nb^{5+} is incorporated into the bulk phase or predominantly resides on the surface. In this context, EDS is commonly utilized, however mostly to solely measure the niobium distribution along the surface. As a matter of fact, considering the studies in which EDS mapping from cross-sectioned particles indicate niobium to be uniformly doped into the bulk phase, there is no agreement in relation to its effect on the material structure.[104,119–124] Moreover, controlling the exact fraction of dopant atoms is challenging and can lead to a loss of active species, resulting in inconsistent structural integrity and electrochemical activity. In relation to the surface doping, inhibition of detrimental surface phenomena and facilitated lithium diffusion are achieved, affecting the CAM capacity minimally, combining to a certain extent the advantages of both bulk doping and coating.[125] Hence, as previously noticed concerning coated materials, a more meticulous analysis involving both the surface and bulk lattice should be considered. It is indeed challenging to precisely describe the interface between coating and doping, and conducting comprehensive studies to assess the effects of different levels of niobium incorporation and gradient characteristics on performance would be complex and demanding.

To illustrate the effects of doping in LTMOs, theoretical studies by means of first-principles simulations have examined niobium as dopant.[108,126,127] Studies with Ni-rich CAMs revealed that it tends to preferentially occupy the octahedral site in the nickel layer, where exchange energies were the lowest. Chen *et al.* simulated NCM811 doping with high-valence ions (V^{5+}, Nb^{5+}, and Zr^{4+}), and it resulted in a decrease in the quantity of nickel ions in a high valence state.[108] The oxidation states of nickel during delithiation were estimated based on calculated magnetic moments and projected density of states (PDOS). At different lithiation levels, the fraction of Ni^{2+} was slightly higher for the doped NCMs compared to the pristine material. Moreover, at low lithium content, the fractions of Ni^{4+} were lower for the doped samples. From these observations, the authors suggest that high-valence dopants can delay the nickel oxidization, being a promising approach in guiding cathode-redox behavior. Apart from that, M–O binding energies in VO_6 (5.2 eV), NbO_6 (6.2 eV), and ZrO_6 (5.7 eV) were found to be higher compared to that in the NiO_6 octahedron (4.3 eV), indicating that V, Nb, and Zr doping serves as a strategy to suppress oxygen evolution.[108] Yoshida *et al.* reported a theoretical study using 32 candidate elements for optimal co-doping with cobalt in LNO in order to improve cycling performance in LIBs.[126] Using an optimized framework, a significant and abrupt decrease in the *c*-axis length was observed during the H2 → H3 transition, suggesting that what actually occurred was a "structural change" rather than a "structural transition". Therefore, a comprehensive screening was performed to identify the optimal doping in LNO able to minimize changes in the *c* parameter. The applied elemental composition ratio was Ni/Co/X = 0.75 : 0.17 : 0.08, where within a unit cell, two nickel sites were substituted by cobalt and one nickel site was occupied by X. Fig. 6a and b represents the screening results, with lower values on the vertical axis indicating reduced contractions (see Fig. 6b). For the descriptors of Δd_{ave}, elemental information on the X substitutes (including atomic numbers, atomic radii, *etc.*) was considered. Among all tested doping elements, bismuth and niobium resulted in the smallest contractions. Nevertheless, the energy required for incorporating bismuth into LNO was found to be notably high, implying the limited ability of bismuth to dissolve efficiently within the structure. Consequently, niobium represented the best-known dopant to mitigate interlayer collapse for LNO and likely for LTMOs in general.

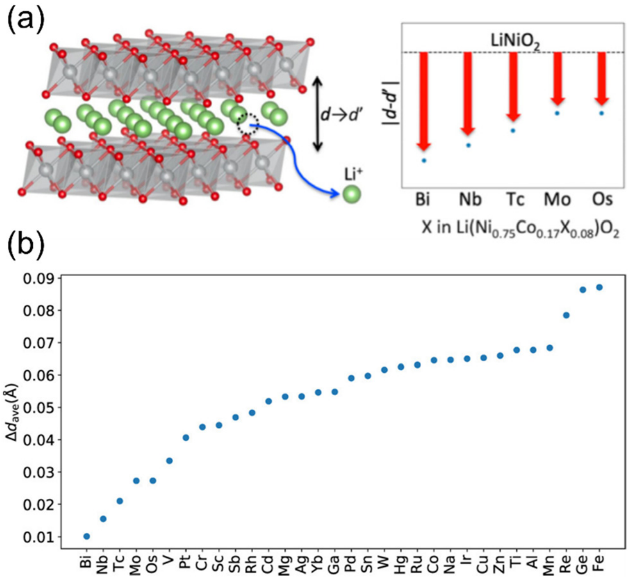

Fig. 6 (a) Representation of layer distance variation as a function of different LNO dopings. (b) Evaluation of *c*-axis contractions induced by 75% charging in terms of Δd_{ave} as a function of doping element. Lower vertical axis values indicate smaller expected contraction and improved cycle performance. Adapted from ref. 126. Copyright 2019, American Chemical Society.

Huang *et al.* used a combination of experimental analyses and first-principles calculations to investigate the effect of Nb-doping on the structure and electrochemical properties of LNO.[112] Pristine and doped LNO were prepared by a solid-state process using $H_5Nb_3O_{10}$ as Nb-dopant precursor. Accordingly, by XRD analysis, Nb^{5+} (1.0 mol%) was found to be uniformly distributed in the LNO structure, occupying the nickel sites and forming a solid solution. Simulated structures revealed that the Nb-doped LNO exhibits a significantly smaller band gap with lower Fermi level, indicating higher conductivity and improved phase stability, respectively, in comparison to the undoped CAM. Theoretical calculations of the migration energy barrier, along with galvanostatic intermittent titration technique (GITT) experiments, revealed that Nb-doping could effectively enhance the diffusion of Li^+ ions within the material.

In fact, experimental observations for Nb-doping and LTMO structure detail situations, where more in-depth analysis is needed. Starting with examples using LNO, Huang *et al.* reported reduced $Ni_{Li}^{\bullet}$ defect fractions based on XRD analysis and lower Ni^{2+} fractions by XPS measurements for the doped material.[112] In contrast, Hao *et al.* also reported Nb-doped LNO prepared under same conditions of temperature, in which $Ni(OH)_2$ spheres were coated using a niobium oxide sol (sol–gel method).[128] In relation to the niobium influence in the CAM structure, its distribution, and effect on electrochemical performance, similar results were obtained. Nevertheless, XRD analysis indicated that Nb-doping causes an increase of the fraction of Ni^{2+}, thereby inducing more $Ni_{Li}^{\bullet}$ defects. Therefore, in relation to the Li^+/Ni^{2+} cation mixing, molar ratio of Ni^{2+}/Ni^{3+}, and Nb^{5+} location in doped LTMO cathodes, different findings are described in the literature. Additional reports of other Ni-rich CAMs support the observed reduction in fraction of $Ni_{Li}^{\bullet}$ defects.[78,104,119,121,129–131] However, these claims contrast with the predicted trend, where high-valence dopants are expected to increase Ni^{2+} content in LTMOs in order to maintain charge balance, facilitating the Li^+/Ni^{2+} cation mixing.[120,122,123,132,133] In this case, considering that Nb-doping is typically carried out concurrently with the lithiation of pCAM, it is likely that Ni^{2+} is not completely oxidized during calcination to maintain charge balance. For instance, the disparity of $Ni_{Li}^{\bullet}$ defects in relation to the base material is illustrated in Fig. 7 (box-and-whisker plot), where a range of negative and positive values can be observed. Furthermore, the variations in specific discharge capacity and cycle retention are shown, which will be discussed below.

In general, the stabilization mechanism of high-valence dopants is more complex.[34] A reduced fraction of $Ni_{Li}^{\bullet}$ defects after Nb-doping was associated with niobium occupancy in TM sites with consequent formation of lithium vacancies.[104] In this mechanism, the substitution of TM sites with Nb^{5+} supposedly occurs without generating any impurity phases (leading to the creation of defects).[104,112] It is crucial to consider that the LTMO lattice has a metal-to-oxygen ratio of 1 : 2, which mismatches the requisite Nb_2O_5 ratio of 1 : 2.5 for an effective doping. It implies that a higher quantity of metal ions is needed to accommodate niobium within the layered structure. This, in turn, implies the demand for additional oxygen. Thus, the oxygen requirement should be fulfilled *via* the gas phase, resulting in the oxidation of the NCM CAM. Moreover, the presence of a considerable concentration of lithium vacancies contributes to a reduced degree of lithiation.

In this context, XPS analysis is usually employed to quantify the content of Ni^{2+} and Ni^{3+} species and make a comparison with the undoped CAM. The common outcomes are the lower fraction of Ni^{2+} as well as the oxidation state of Nb^{5+} and the stronger Nb–O bonds for doped materials.[78,112,119,131,134] However, as mentioned previously in relation to coatings, XPS is a surface-based technique, which has a penetration depth of only 10–20 atomic layers.[135] Therefore, XPS cannot be used as a prescription for the nature of the bulk of doped LTMO, rather it is a complementary technique to others. Chu *et al.* showed that the fraction of $Ni_{Li}^{\bullet}$ defects initially decreases and then increases with the incorporation of more niobium in NCM811 (0, 1, and 3 wt%).[121] EDS mapping from cross-sectioned particles of the most concentrated sample (3 wt%) confirmed that niobium was uniformly doped into the bulk phase. XPS results indicated that increasing the Nb-doping level leads to a corresponding increase in the ratio of Ni^{2+}/Ni^{3+}, while the valences of manganese and cobalt did not change. To explore the positioning of niobium within the lattice of the doped NCM samples, the authors conducted a combined analysis of NPD and XRD. Curiously, the results revealed a most likely structural model containing niobium in the octahedral sites of both the TM and lithium layers. Apart from that, reports of $LiNi_{0.8}Co_{0.2}O_2$[136] and $Li_{1.2}Mn_{0.54}Ni_{0.13}Co_{0.13}O_2$[137] describe niobium only in the lithium position, with slightly decreased and no changes in cell parameters, respectively. In the first report, this assumption is based only on XRD data, and no further evidence was provided. In the second report, Liu *et al.* proposed the presence of Nb^{5+} in the lithium layer near the surface, utilizing high-angle annular dark-field (HAADF) and annular bright-field (ABF) STEM images, based on color contrast proportionate to atomic number, as shown in Fig. 8.[137] However, it is worth considering that such image contrast could also suggest the presence of Ni^{2+} rather than Nb^{5+} in the lithium site. For instance, comparable findings in other studies indeed offer evidence of disordered phase formation, attributed to Ni^{2+} occupying the lithium site.[138–140] The authors also considered density functional theory (DFT) calculations to support the preferred occupancy of niobium.[137] Yet, other reports of LTMO CAMs with similar composition (high Mn-content) describe niobium located in either TM position[141,142] or specifically in Ni[124] or Mn[117] sites. As high-

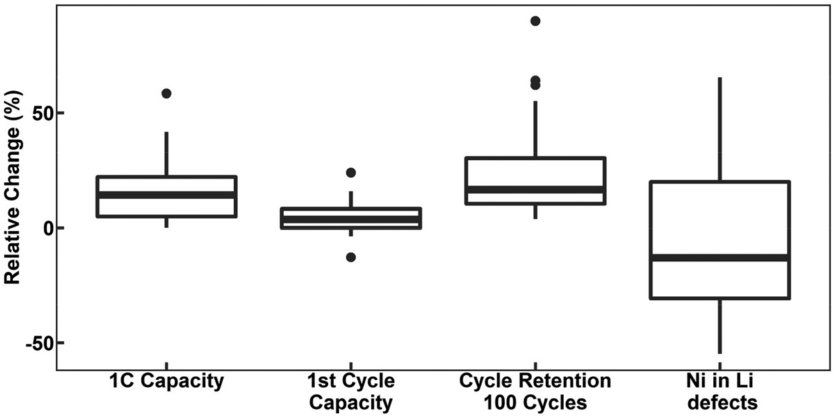

Fig. 7 Box-and-whisker plot of the relative change of 1C capacity (*n* = 16), first-cycle capacity (*n* = 22), capacity retention after 100 cycles (*n* = 22), and $Ni_{Li}^{\bullet}$ defects (*n* = 11) of Nb-doped LTMOs applied for LIBs.

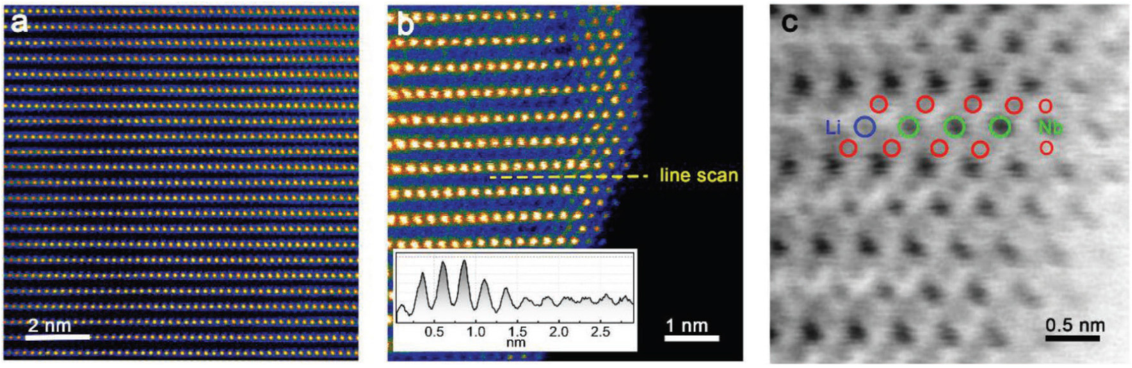

Fig. 8 STEM images of Nb-doped $Li_{1.2}Mn_{0.54}Ni_{0.13}Co_{0.13}O_2$. (a) HAADF image of the bulk. (b) HAADF image of the surface near region. (c) ABF-enlarged image of the surface shown in panel (b). Adapted from ref. 137. Copyright 2018, Wiley-VCH GmbH.

lighted previously, these variances can be related to the applied synthesis conditions and particularly to the lack of more detailed investigation. Interestingly, from all references claiming Nb-doping in this review, the study by Liu *et al.* is unique in using niobium ethoxide as precursor (a known precursor and procedure for coating purposes), which was mixed to the LTMO and annealed at 600 °C for 6 h.[137] Moreover, their findings indicated a surface rather than a bulk doping. Therefore, it can be inferred that a possible additional coating should be considered in this case, and the surface doping is a consequence of the applied temperature, as discussed before. A potential increase in Ni^{2+} concentration within doped LTMOs could likely be correlated with the formation of rock-salt type NiO, stemming from the insertion of Nb^{5+}, which leads to Li^+ consumption and oxygen release. What is clear by the standing literature is the uncertainty of where niobium sits in LTMOs, whether there really is a dependency on TM choice (Ni-rich or Mn-rich), what the solubility limit is for niobium inclusion, and its effects on $Ni^{\bullet}_{Li}$ defects.

Single crystal (SC) LTMOs are another category of materials being researched for LIBs. Particularly with the increasing popularity of SSBs, they have gained interest as a natural complement to this platform, yet doping in either context is lacking. Single-crystalline LTMOs are ideally composed of individual crystallites but practically consist of 3–5 agglomerated grains.[143] As noted elsewhere,[144] increasing particle (grain) size leads to a reduction in surface area per unit mass, which helps mitigate surface reactions and whose deagglomerated character can alleviate the issue of intergranular cracking commonly observed in polycrystalline NCM CAMs. Nevertheless, they present balance of limitations related to an increased path length for lithium diffusion. In this context, controlling diffusivity becomes crucial, as higher diffusivity enables the use of larger particles, thereby reducing the occurrence of surface-based degradation. Zhang *et al.* showed the effects of high-valence ions (*e.g.*, Nb^{5+} and Y^{3+}) when applied to dope SC NCM.[145] The doped NCM712 was prepared by adding respective precursors to pCAM and LiOH, and then sintering the material under proper conditions (480 °C for 6 h and 930 °C for 15 h, in O_2 atmosphere). For the Nb-doped NCM, EDS of cross-sectioned particles demonstrated a uniform distribution of niobium throughout the entire single-crystalline particles. At both room and high temperatures, the Nb-doped SC NCM cathode exhibited the best electrochemical performance among the tested materials. The significant enhancement was attributed to a possible occupation of niobium at the lithium site. In contrast, small increases in cell parameters observed by XRD were ascribed to the larger ionic radius of niobium compared to the TMs in the NCM. Nevertheless, this would only be reasonable if the doping occurred at the TM sites, given that Li^+ is larger than the Nb^{5+} ion. In addition, the XRD analysis also indicated a lower fraction of $Ni^{\bullet}_{Li}$ defects after doping.[145] This was associated with XPS results, in which the authors suggested that the peak positions could be attributed to Nb^{4+} and Nb^{5+} and therefore Nb-doping would promote the oxidation of Ni^{2+} to Ni^{3+}, contradicting the other reports. Moreover, it is important to note that differentiating between Nb^{4+} and Nb^{5+} using XPS exclusively is challenging due to the proximity of their binding-energy values. Discrepancies for the corresponding values of the $3d_{3/2}$ and $3d_{5/2}$ states of Nb^{5+} are typical in the literature and are likely attributed to varying chemical environments rather than a genuine change in oxidation state.[146]

Indeed, inconsistencies and contrasting results are also present in studies involving SC CAMs. For instance, Zhao *et al.* investigated the impact of Nb-doping on $Ni^{\bullet}_{Li}$ defects, suggesting its potential regulatory effect.[123] They considered that a proper cation mixing could enhance the lithium transport and prevent NCM lattice collapse during deep delithiation. Commercial SC NCM811 was doped by ball milling it with $LiNbO_3$ and LiOH, followed by subsequent calcination (500 °C for 4 h and 750 °C for 12 h, in O_2 atmosphere). Combining the results obtained by electron backscatter diffraction (EBSD), EDS, time-of-flight secondary ion mass spectrometry (ToF-SIMS), NPD, XRD, and XAS, Nb^{5+} was observed to occupy 3b sites (most probably nickel site), be uniformly distributed, and to provoke a higher Li^+/Ni^{2+} cation mixing. As a result, *c* parameter and average lattice fringe spacing increased, which is advantageous for the lithium transport within the channels.[123] Furthermore, through DFT calculations, it was observed that the introduction of niobium modulates the SC NCM band gap and enhances the electronic conductivity. Jamil *et al.* observed similar results when mixing Nb_2O_5 to a NCM811 pCAM with LiOH and further sintering the material (750 °C for 20 h, in O_2 atmosphere).[122] The strong binding force of Nb–O contributed to the stabilization of lattice oxygen, while the high valence of Nb^{5+} increased the occurrence of $Ni_{Li}^{\bullet}$ defects, leading to the formation of a protective disordered rock-salt layer on the surface. In contrast, Wu *et al.* showed some different results, even though NCM with comparable composition (NCM831205) and similar experimental conditions were applied.[129] A distinct linear concentration gradient of Nb-doping was observed by EDS and depth-dependent XPS (ion etching), with the concentration of niobium progressively decreasing from the particle surface towards its core. Both the surface and the internal region of doped sample exhibited an ordered layered structure. However, pristine NCM displayed a rock-salt type structure on its surface with a thickness ranging from 2 to 4 nm. For the doped sample, its surface exhibited more Ni^{3+} species, which resulted in a lower fraction of $Ni_{Li}^{\bullet}$ defects. Consequently, a higher concentration of Co^{2+} was observed and attributed to the conversion of some Co^{3+} species in order to maintain the overall charge balance.

In summary, the literature generally relies on a combination of X-ray and microscopy techniques to physically characterize Nb-doped CAMs. However, other techniques that could provide valuable insights into the structural character of niobium in LTMOs are often not included. Concerning the crystallographic structure, Nb-doped layered oxide cathodes show the expected α-$NaFeO_2$ structure and $R\bar{3}m$ space group as pristine LTMO materials. As mentioned earlier, XRD patterns are commonly analyzed by Rietveld refinement, and changes in Li^+/Ni^{2+} cation mixing are reported using this method. TEM analysis usually serves to confirm the regular layered lattice and the enlargement of interplanar spacing after doping. Nevertheless, lattice parameters are typically key indicators of niobium incorporation, in which changes related to its relatively large ionic radius, in particular an expansion of cell volume and the *c*-axis (metal–metal interslab distance), are the main observations. These variations can become irregular when new phases are formed (Li_3NbO_4, $LiNbO_3$, Nb_2O_5).[116] Indeed, it is worth highlighting that the ion size of Nb^{5+} is not notably larger, especially in comparison to the Ni^{2+} radius. Furthermore, literature will almost exclusively measure materials using "lab-scale" diffraction instruments, which have limited resolution for such a small structural deviation, yet will report R_{wp} values that require very careful material preparation (*i.e.*, proper packing of capillary for Debye–Scherrer diffraction), external instrument calibration (*i.e.*, NIST LaB_6), and internal Si standards to account for displacement errors, all of which is generally unheard of for battery research groups to report. Synchrotron XRD measurements are a better option to regular XRD (synchrotron results were recently reported by Xin *et al.*, for example).[59] Nb-modified NCM9055 was prepared by firstly coating the pCAM [$Ni_{0.9}Co_{0.05}Mn_{0.05}(OH)_2$] using niobium ethoxide, and then calcining it with LiOH (725 °C). The increasing niobium concentration in NCM9055 resulted in the appearance of extra peaks, indicating the formation of Li_3NbO_4. The lattice parameters were slightly expanded, and the relative intensity between (003)/(104) reflections, an indicator of Li^+/Ni^{2+} cation mixing, showed minor changes with increasing niobium concentration (from 1.59 for pristine to 1.49 for 2.1 at% Nb-NCM).[59] Nevertheless, it is noteworthy to mention that this method based on peak intensities is generally unreliable and should be avoided.[8] Moreover, additional X-ray techniques are possible but, for the purported promise of niobium and "need" to understand its role in LTMOs, their use is conspicuously absent. For instance, X-ray absorption near-edge structure (XANES) is well suited for determining oxidation states and coordination chemistry (*e.g.*, octahedral or tetrahedral geometry), while extended X-ray absorption fine structure (EXAFS) offers a method to determine local structure, coordination number, and environment (niobium position).[147] Pair distribution function (PDF) technique could be similarly applied to determine local structure.[148] Alternatively, magnetic characterization can provide a complementary method to determine Li^+/Ni^{2+} cation mixing character, as the presence of excess Ni^{2+} in the lithium layer is known to be correlated with magnetic ordering and the coupling of different nickel layers.[149,150] Xin *et al.* showed magnetic susceptibility studies for Nb-modified NCM exposed to different temperatures. The Curie–Weiss behavior exhibited a magnetic transition at 10 K in pristine and doped NCM samples treated at 400 and 500 °C. However, for the materials treated at higher temperatures, the transition shifted to 11.5 K, providing confirmation of lattice modification through niobium substitution.[35] Furthermore, solid-state nuclear magnetic resonance (NMR) spectroscopy using ^{93}Nb and $^{6}Li/^{7}Li$ could be a relatively accessible method to characterize the nature of niobium in LTMOs.[151] At this time, there are no known reports using either nucleus to characterize Nb-doped (or coated) CAMs. This does not necessarily imply that these techniques should be standard practice, but rather emphasizes the importance of conducting such studies to gain a deeper understanding of how niobium influences the local and bulk structure of LTMO. By doing so, more informed observations and hypotheses can be put forth when the field publishes a series of reports on Nb-doping with slightly different NCM stoichiometries.

In regards to more routine measurements, EDS can see the incorporation depth and surface distribution of niobium, as mentioned before. Additionally, differential scanning calorimetry (DSC) has been applied to show that Nb-doping enhances the thermal stability of the material, particularly for Ni-rich CAMs.[122,129,130,136,152] In fact, several studies have demonstrated improved cyclability for Nb-doped NCMs at elevated temperatures (45–60 °C) compared to their pristine counterparts.[78,120,122,124,128,136,145,152] For instance, Nb-doping (1 mol%) could increase the capacity retention of NCM831106 at 60 °C from ~20% to almost 72% after 200 cycles.[120] In general, this enhancement is correlated to the better structural stability offered by the Nb-modified LTMO.[120,122,124,145] Hao *et al.* investigated the electrochemical performance of Nb-doped LNO (1 mol%) at different temperatures (55 to −10 °C), where side reactions at the electrode/electrolyte interface were diminished, especially at higher temperatures, thereby enhancing interfacial stability during cycling.[128] Apart from that, EIS suggested faster lithium diffusion, even at low temperature. In relation to the material morphology and particle size, no significant changes are generally reported for secondary particles by comparing SEM images before and after doping.[112,129,130,136,152] On the other hand, when the primary particles are compared, niobium appears to cause a significant reduction in their sizes.[59,119,120,128,153] Park *et al.* showed an interesting study in this regard using different high-valence elements (Al^{3+}, Nb^{5+}, Ta^{5+}, and Mo^{6+}) to dope LNO.[115] The samples were prepared by mixing $Ni(OH)_2$, LiOH, and dopant precursor, with further calcination within the temperature range of 650 to 800 °C. Changes in primary particle morphology were carefully analyzed by cross-sectional SEM images. While Al-doped LNO displayed similar coarsening behavior to undoped material and maintained its particle shape, primary particles of Nb-, Ta-, and Mo-doped LNO exhibited smaller particle sizes and maintained a radial alignment at each temperature. Fig. 9 displays the cross-sectional images of Nb-LNO compared to LNO. In addition, *in situ* XRD analysis revealed that the dopants formed Li–X–O compounds when introduced to the samples. In the case of Nb-LNO, distinct reflections of $LiNbO_3$ at temperatures between 450 and 730 °C were identified. At higher temperatures, the peaks gradually weakened and the Li_3NbO_4 phase emerged, remaining stable up to 750 °C. The presence of Li–X–O compounds during high-temperature calcination resulted in grain-boundary coating, inhibiting boundary migration and suppressing primary particle coarsening. Therefore, the mechanism of doping high-valence ions into LNO involved not only bulk incorporation but also grain-boundary coating, affecting the microstructure. The highest discharge capacity was achieved when the cathodes were calcined at 680–700 °C. Ober *et al.* also reported a similar finding, where the formation of intergranular Li_xNbO_y phases in LNO impeded the growth of its primary particles.[153] Hence, as previously emphasized, temperature conditions significantly influence niobium modification of LTMOs, and the possibility of an additional coating on the particle surface, including the primary particles themselves, should be considered.

The electrochemical performance of Nb-doped LTMOs shows empirically that there is a significant improvement above the "baseline" material often referenced. Evaluation of cycling (galvanostatic or voltammetric), EIS, and differential capacity analysis are the cornerstone techniques applied and provide much of the basis for the trends observed, however are not the only techniques that should be used, as including physical characterization is very insightful. For example, *operando* XRD studies during the first charge process demonstrated a smooth reversibility of H2 → H3 phase transition with a significant suppression of the lattice contraction in Nb-doped samples.[121–123] Nb-doping (and coating) also seems to inhibit or mitigate oxygen release, as demonstrated by *operando* differential electrochemical mass spectrometry (DEMS).[123,124,154] *Post-mortem* characterization comprises of easy-to-access SEM, TEM, XRD, and XPS. Microscopy images, in particular from cross sections, serve as an evidence of lower cracking and the better mechanical integrity of doped CAMs.[59,112,119,121,145] XRD patterns show less lattice distortion and even less $Ni_{Li}^{\bullet}$ defects after cycling for the doped sample.[129] As to the composition of cycled electrodes, XPS exhibited reduced Ni^{2+} formation and lower content of impurities related to the CEI formation or carbonates.[104,122,129]

Based on our meta-analysis, Nb-doping significantly enhances the performance of LTMOs, as shown in Table 2 and Fig. 7. With regards to capacity, Nb-doping did not have a significant impact with a median relative change of 3.7%. In some reports, the introduction of niobium results in increased values of initial discharge capacity. This enhancement is generally attributed to the diffusion of lithium ions, which is facilitated by the decreased fraction of $Ni_{Li}^{\bullet}$ defects and the for-

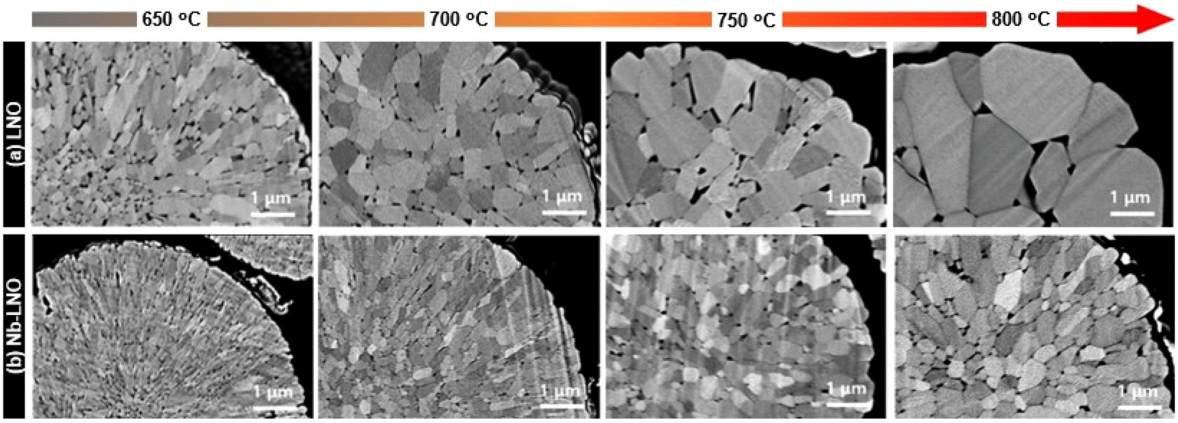

Fig. 9 Cross-sectional SEM images of (a) as-prepared LNO and (b) Nb-LNO calcined at 650–800 °C. Adapted from ref. 115. Copyright 2023, Wiley-VCH GmbH.

mation of lithium vacancies.[104,121,137,142] In the same way, the initial Coulomb efficiency is also enhanced as a result of an improved structural stability and reduced irreversible Li^+ extraction.[104,137] However, other works reported a decreased discharge capacity for the Nb-doped CAM and associated it to the introduction of inactive Nb^{5+} ions in TM sites and higher $\text{Li}^+/\text{Ni}^{2+}$ cation mixing.[78,112,116,120] As mentioned earlier, the true effect that Nb-doping has on $\text{Ni}_{\text{Li}}^{\bullet}$ defects is not fully understood yet; there is a moderate decrease in the concentration of such defects at a median relative change of −13.0% (see Fig. 7). Caution should be taken as to the veracity of this claim based on the previously reported reasons. This is because the Ni^{2+} levels in Nb-doped LTMOs may be linked to the choice of niobium precursor and preparation method or could potentially result from insufficient characterization. Therefore, if additional supporting evidence emerges in the future, it should be duly reported. Across a range of cycle numbers, from 45 to 300, the capacity retention shows the most notable improvement in all cases, with distinct niobium precursors and concentrations. The number of 100 cycles is a commonly used benchmark in the literature to demonstrate electrochemical stability. Taking this into account and considering the values of the respective materials before doping, there is a moderate increase in median rate capability (1C = 14.3%) and cycle stability (100 cycles = 16.7%). Regardless, this improved performance of Nb-doped LTMOs can be attributed to the several factors discussed before, particularly the enhancement of internal stability, facilitated lithium diffusion, better electronic conductivity and therefore reduced polarization. These combined effects also result in a robust electrochemical stability even under high current density and voltage conditions.[78,121,122,134]

4. Conclusions and outlook

In conclusion, the role of niobium in Li-based LTMO cathodes is manifold and influenced by various factors, such as synthesis conditions, precursor selection, and its concentration with regard to the CAM. In relation to Nb-based coating, LiNbO_3 has emerged as the most prominent example, due to its ease of synthesis and positive electrochemical performance characteristics. It effectively reduces metal dissolution and contributes significantly to cycle retention and rate capability. Nevertheless, it is important to employ complementary characterization techniques and consider factors, such as physical thickness, rather than reported molar or weight percentage, to better understand material performance. Moreover, as has been recognized recently in the literature, it seems that pure LiNbO_3 coatings are difficult to achieve, the morphology strongly depends on the synthesis conditions, and often carbonate species are incorporated. This makes the analysis of structure–composition relationships challenging. Regarding Nb-based doping, an important consideration is the impact of the preparation method on the final product, with annealing conditions and concentration playing pivotal roles in material modification. In general, XRD is the most commonly used technique to investigate doping and its influence on the structure of the base material. However, more meticulous characterizations are mostly needed. Through the analysis of several studies, most of the reports have indicated Nb^{5+} location in the nickel site. Nevertheless, there is still no agreement regarding its effects, particularly concerning the Ni^{2+} concentration and $\text{Ni}_{\text{Li}}^{\bullet}$ point defects after doping. In this regard, the increased Ni^{2+} content might be correlated to the formation of rock-salt type NiO through lithium consumption and oxygen release, or even to incomplete oxidation when niobium is introduced during the lithiation of pCAM. However, the precise doping mechanism remains unclear and could also be associated to the formation of lithium vacancies. Apart from that, there is often no clear differentiation between surface and bulk doping, and a possible additional coating formation is not considered. Distinguishing between doping and coating can be challenging, and the detection of additional coatings in Nb-doped materials is often unclear due to their minimal concentration and widespread distribution. Regardless, the beneficial impact of niobium modification on the electrochemical performance of LTMO cathodes is evident and is generally related to the enhancement of stability, facilitated lithium diffusion, better electronic conductivity, and reduced polarization. In future studies, a more in-depth investigation into the specific location and behavior of niobium in Li-based CAMs is recommended. This will enable the development of enhanced battery materials by harnessing the benefits of Nb-based doping and coating, ultimately advancing the performance and stability of LIBs and SSBs.

Conflicts of interest

There are no conflicts to declare.

Acknowledgements

This work was supported by BASF SE. The authors are grateful to the Federal Ministry of Education and Research (Bundesministerium für Bildung und Forschung, BMBF) for funding within the projects SUSTRAB (03XP0415D), UNIKAM (03XP0484B), and MELLi (03XP0447).

References

1 J.-M. Tarascon and M. Armand, Issues and challenges facing rechargeable lithium batteries, *Nature*, 2001, **414**, 359–367.

2 J. B. Goodenough and Y. Kim, Challenges for rechargeable Li batteries, *Chem. Mater.*, 2010, **22**, 587–603.

3 K. Mizushima, P. C. Jones, P. J. Wiseman and J. B. Goodenough, Li_xCoO_2 $(0 < x < -1)$: A new cathode material for batteries of high energy density, *Mater. Res. Bull.*, 1980, **15**, 783–789.

4 M. S. Whittingham, Lithium batteries and cathode materials, *Chem. Rev.*, 2004, **104**, 4271–4302.

5 G. A. Campbell, The cobalt market revisited, *Miner. Econ.*, 2020, **33**, 21–28.

6 Y. Kim, W. M. Seong and A. Manthiram, Cobalt-free, high-nickel layered oxide cathodes for lithium-ion batteries: Progress, challenges, and perspectives, *Energy Storage Mater.*, 2021, **34**, 250–259.

7 H.-J. Noh, S. Youn, C. S. Yoon and Y.-K. Sun, Comparison of the structural and electrochemical properties of layered $Li[Ni_xCo_yMn_z]O_2$ (x = 1/3, 0.5, 0.6, 0.7, 0.8 and 0.85) cathode material for lithium-ion batteries, *J. Power Sources*, 2013, **233**, 121–130.

8 M. Bianchini, M. Roca-Ayats, P. Hartmann, T. Brezesinski and J. Janek, There and back again—The journey of $LiNiO_2$ as a cathode active material, *Angew. Chem., Int. Ed.*, 2019, **58**, 10434–10458.

9 H. H. Sun, H.-H. Ryu, U.-H. Kim, J. A. Weeks, A. Heller, Y.-K. Sun and C. B. Mullins, Beyond doping and coating: Prospective strategies for stable high-capacity layered Ni-rich cathodes, *ACS Energy Lett.*, 2020, **5**, 1136–1146.

10 Z. Ye, L. Qiu, W. Yang, Z. Wu, Y. Liu, G. Wang, Y. Song, B. Zhong and X. Guo, Nickel-rich layered cathode materials for lithium-ion batteries, *Chem. – Eur. J.*, 2021, **27**, 4249–4269.

11 R. Jung, M. Metzger, F. Maglia, C. Stinner and H. A. Gasteiger, Oxygen release and its effect on the cycling stability of $LiNi_xMn_yCo_zO_2$ (NMC) cathode materials for Li-ion batteries, *J. Electrochem. Soc.*, 2017, **164**, A1361–A1377.

12 F. Strauss, J. H. Teo, A. Schiele, T. Bartsch, T. Hatsukade, P. Hartmann, J. Janek and T. Brezesinski, Gas evolution in lithium-ion batteries: Solid versus liquid electrolyte, *ACS Appl. Mater. Interfaces*, 2020, **12**, 20462–20468.

13 L. de Biasi, B. Schwarz, T. Brezesinski, P. Hartmann, J. Janek and H. Ehrenberg, Chemical, structural, and electronic aspects of formation and degradation behavior on different length scales of Ni-rich NCM and Li-rich HE-NCM cathode materials in Li-ion batteries, *Adv. Mater.*, 2019, **31**, 1900985.

14 D. J. Xiong, T. Hynes, L. D. Ellis and J. R. Dahn, Effects of surface coating on gas evolution and impedance growth at $Li[Ni_xMn_yCo_{1-x-y}]O_2$ positive electrodes in Li-ion cells, *J. Electrochem. Soc.*, 2017, **164**, A3174–A3181.

15 S. L. Dreyer, A. Kondrakov, J. Janek and T. Brezesinski, In situ analysis of gas evolution in liquid- and solid-electrolyte-based batteries with current and next-generation cathode materials, *J. Mater. Res.*, 2022, **37**, 3146–3168.

16 A. O. Kondrakov, A. Schmidt, J. Xu, H. Geßwein, R. Mönig, P. Hartmann, H. Sommer, T. Brezesinski and J. Janek, Anisotropic lattice strain and mechanical degradation of high- and low-nickel NCM cathode materials for Li-ion batteries, *J. Phys. Chem. C*, 2017, **121**, 3286–3294.

17 A. O. Kondrakov, H. Geßwein, K. Galdina, L. de Biasi, V. Meded, E. O. Filatova, G. Schumacher, W. Wenzel, P. Hartmann, T. Brezesinski and J. Janek, Charge-transfer-induced lattice collapse in Ni-rich NCM cathode materials during delithiation, *J. Phys. Chem. C*, 2017, **121**, 24381–24388.

18 D. Weber, Đ. Tripković, K. Kretschmer, M. Bianchini and T. Brezesinski, Surface modification strategies for improving the cycling performance of Ni-rich cathode materials, *Eur. J. Inorg. Chem.*, 2020, 3117–3130.

19 P. Guan, L. Zhou, Z. Yu, Y. Sun, Y. Liu, F. Wu, Y. Jiang and D. Chu, Recent progress of surface coating on cathode materials for high-performance lithium-ion batteries, *J. Energy Chem.*, 2020, **43**, 220–235.

20 C. Nico, T. Monteiro and M. P. F. Graça, Niobium oxides and niobates physical properties: Review and prospects, *Prog. Mater. Sci.*, 2016, **80**, 1–37.

21 W. M. Haynes, *CRC Handbook of Chemistry and Physics*, CRC Press, 2014.

22 S.-J. Sim, S.-H. Lee, B.-S. Jin and H.-S. Kim, Improving the electrochemical performances using a V-doped Ni-rich NCM cathode, *Sci. Rep.*, 2019, **9**, 8952.

23 R. Zhu, Y. Wang, Y. Han, Y. Huang, M. Zhang, X. Lai, Z. Yang and Z. Li, Internal and external bifunctional vanadium-modification strategy for $LiNi_{0.80}Co_{0.15}Al_{0.05}O_2$ cathode materials, *Ceram. Int.*, 2023, **49**, 5169–5179.

24 L. Cai, Q. Han, Z. Yang, Y. Hu, H. Jiang and C. Li, In situ co-modification strategy for achieving high-capacity and durable Ni-rich cathodes for high-temperature Li-ion batteries, *Energy Fuels*, 2022, **36**, 12319–12326.

25 B. Chu, S. Liu, L. You, D. Liu, T. Huang, Y. Li and A. Yu, Enhancing the cycling stability of Ni-rich $LiNi_{0.6}Co_{0.2}Mn_{0.2}O_2$ cathode at a high cutoff voltage with Ta doping, *ACS Sustainable Chem. Eng.*, 2020, **8**, 3082–3090.

26 S. Jamil, R. Yu, Q. Wang, M. Fasehullah, Y. Huang, Z. Yang, X. Yang and X. Wang, Enhanced cycling stability of nickel-rich layered oxide by tantalum doping, *J. Power Sources*, 2020, **473**, 228597.

27 X. Zhang, P. Zhang, T. Zeng, Z. Yu, X. Qu, X. Peng, Y. Zhou, X. Duan, A. Dou, M. Su and Y. Liu, Improving the structure stability of $LiNi_{0.8}Co_{0.15}Al_{0.05}O_2$ by double modification of tantalum surface coating and doping, *ACS Appl. Energy Mater.*, 2021, **4**, 8641–8652.

28 F. A. Susai, D. Kovacheva, A. Chakraborty, T. Kravchuk, R. Ravikumar, M. Talianker, J. Grinblat, L. Burstein, Y. Kauffmann, D. T. Major, B. Markovsky and D. Aurbach, Improving performance of $LiNi_{0.8}Co_{0.1}Mn_{0.1}O_2$ cathode materials for lithium-ion batteries by doping with molybdenum-ions: Theoretical and experimental studies, *ACS Appl. Energy Mater.*, 2019, **2**, 4521–4534.

29 O. Breuer, A. Chakraborty, J. Liu, T. Kravchuk, L. Burstein, J. Grinblat, Y. Kauffman, A. Gladkih, P. Nayak, M. Tsubery, A. I. Frenkel, M. Talianker, D. T. Major, B. Markovsky and D. Aurbach, Understanding the role of minor molybdenum doping in $LiNi_{0.5}Co_{0.2}Mn_{0.3}O_2$ electrodes: From structural and surface analyses and theoretical modeling to practical electrochemical cells, *ACS Appl. Mater. Interfaces*, 2018, **10**, 29608–29621.

30 L. Liang, X. Li, M. Su, L. Wang, J. Sun, Y. Liu, L. Hou and C. Yuan, Chemomechanically stable small single-crystal Mo-doped $LiNi_{0.6}Co_{0.2}Mn_{0.2}O_2$ cathodes for practical 4.5 V-class pouch-type Li-ion batteries, *Angew. Chem., Int. Ed.*, 2023, **62**, e202216155.

31 D. Gao, Y. Huang, H. Dong, C. Li and C. Chang, Atomic horizons interpretation on enhancing electrochemical performance of Ni-Rich NCM cathode via W doping: Dual improvements in electronic and ionic conductivities from DFT calculations and experimental confirmation, *Small*, 2023, **19**, 2205122.

32 R. Zhang, H. Qiu and Y. Zhang, Enhancing the electrochemical performance of Ni-rich $LiNi_{0.88}Co_{0.09}Al_{0.03}O_2$ cathodes through tungsten-doping for lithium-ion batteries, *Nanomaterials*, 2022, **12**, 729.

33 J. Wang, C. Liu, Q. Wang, G. Xu, C. Miao, M. Xu, C. Wang and W. Xiao, Investigation of W^{6+}-doped in high-nickel $LiNi_{0.83}Co_{0.11}Mn_{0.06}O_2$ cathode materials for high-performance lithium-ion batteries, *J. Colloid Interface Sci.*, 2022, **628**, 338–349.

34 Z. Ahaliabadeh, X. Kong, E. Fedorovskaya and T. Kallio, Extensive comparison of doping and coating strategies for Ni-rich positive electrode materials, *J. Power Sources*, 2022, **540**, 231633.

35 F. Xin, H. Zhou, Y. Zong, M. Zuba, Y. Chen, N. A. Chernova, J. Bai, B. Pei, A. Goel, J. Rana, F. Wang, K. An, L. F. J. Piper, G. Zhou and M. S. Whittingham, What is the role of Nb in nickel-rich layered oxide cathodes for lithium-ion batteries?, *ACS Energy Lett.*, 2021, **6**, 1377–1382.

36 P. Heitjans, M. Masoud, A. Feldhoff and M. Wilkening, NMR and impedance studies of nanocrystalline and amorphous ion conductors: Lithium niobate as a model system, *Faraday Discuss.*, 2007, **134**, 67–82.

37 H. Franke, *Physica status solidi/A*, De Gruyter, 1983, vol. 83, pp. 493–496.

38 A. V. Yatsenko, S. V. Yevdokimov and A. A. Yatsenko, Analysis of the ionic contribution to the electrical conductivity of $LiNbO_3$ crystals, *Ferroelectrics*, 2021, **576**, 157–162.

39 Y. Ito and I. Tsuyumoto, Preparation of nanocrystalline $LiNbO_3$ through aqueous solution process using peroxopolyniobic acid, *Mater. Chem. Phys.*, 2021, **272**, 125035.

40 A. M. Glass, K. Nassau and T. J. Negran, Ionic conductivity of quenched alkali niobate and tantalate glasses, *J. Appl. Phys.*, 1978, **49**, 4808–4811.

41 N. Ohta, K. Takada, I. Sakaguchi, L. Zhang, R. Ma, K. Fukuda, M. Osada and T. Sasaki, $LiNbO_3$-coated $LiCoO_2$ as cathode material for all solid-state lithium secondary batteries, *Electrochem. Commun.*, 2007, **9**, 1486–1490.

42 G. Hu, Y. Tao, Y. Lu, J. Fan, L. Li, J. Xia, Y. Huang, Z. Zhang, H. Su and Y. Cao, Enhanced electrochemical properties of $LiNi_{0.8}Co_{0.1}Mn_{0.1}O_2$ cathode materials modified with lithium-ion conductive coating $LiNbO_3$, *ChemElectroChem*, 2019, **6**, 4773–4780.

43 A. Guéguen, D. Streich, M. He, M. Mendez, F. F. Chesneau, P. Novák and E. J. Berg, Decomposition of $LiPF_6$ in high energy lithium-ion batteries studied with online electrochemical mass spectrometry, *J. Electrochem. Soc.*, 2016, **163**, A1095–A1100.

44 E. Peled, The electrochemical behavior of alkali and alkaline earth metals in nonaqueous battery systems—The solid electrolyte interphase model, *J. Electrochem. Soc.*, 1979, **126**, 2047–2051.

45 K. Xu, Interfaces and interphases in batteries, *J. Power Sources*, 2023, **559**, 232652.

46 K. Xu, Nonaqueous liquid electrolytes for lithium-based rechargeable batteries, *Chem. Rev.*, 2004, **104**, 4303–4417.

47 L. Benitez and J. M. Seminario, Ion diffusivity through the solid electrolyte interphase in lithium-ion batteries, *J. Electrochem. Soc.*, 2017, **164**, E3159–E3170.

48 S. Shi, Y. Qi, H. Li and L. G. Hector, Defect thermodynamics and diffusion mechanisms in Li_2CO_3 and implications for the solid electrolyte interphase in Li-ion batteries, *J. Phys. Chem. C*, 2013, **117**, 8579–8593.

49 K. Tasaki, A. Goldberg, J.-J. Lian, M. Walker, A. Timmons and S. J. Harris, Solubility of lithium salts formed on the lithium-ion battery negative electrode surface in organic solvents, *J. Electrochem. Soc.*, 2009, **156**, A1019–A1027.

50 S.-J. Kwon, S.-E. Lee, J.-H. Lim, J. Choi and J. Kim, Performance and life degradation characteristics analysis of NCM LIB for BESS, *Electronics*, 2018, **7**, 406.

51 S. Wenzel, T. Leichtweiss, D. A. Weber, J. Sann, W. G. Zeier and J. Janek, Interfacial reactivity benchmarking of the sodium ion conductors Na_3PS_4 and sodium β-alumina for protected sodium metal anodes and sodium all-solid-state batteries, *ACS Appl. Mater. Interfaces*, 2016, **8**, 28216–28224.

52 S. P. Culver, R. Koerver, W. G. Zeier and J. Janek, On the functionality of coatings for cathode active materials in thiophosphate-based all-solid-state batteries, *Adv. Energy Mater.*, 2019, **9**, 1900626.

53 J. H. Kim, H. Kim, W. Choi and M. S. Park, Bifunctional surface coating of $LiNbO_3$ on high-Ni layered cathode materials for lithium-ion batteries, *ACS Appl. Mater. Interfaces*, 2020, **12**, 35098–35104.

54 W. Cho, S.-M. Kim, J. H. Song, T. Yim, S.-G. Woo, K.-W. Lee, J.-S. Kim and Y.-J. Kim, Improved electrochemical and thermal properties of nickel rich $LiNi_{0.6}Co_{0.2}Mn_{0.2}O_2$ cathode materials by SiO_2 coating, *J. Power Sources*, 2015, **282**, 45–50.

55 L. Dou, A. Tang, W. Lin, X. Dong, L. Lu, C. Shang, Z. Zhang, Z. Huang, K. Aifantis, P. Hu and D. Xiao, Enhancing the electrochemical performance of $LiNi_{0.8}Co_{0.1}Mn_{0.1}O_2$ cathodes through amorphous coatings, *Electrochim. Acta*, 2022, **425**, 140745.

56 B. Wang, H. Zhao, F. Cai, Z. Liu, G. Yang, X. Qin and K. Świerczek, Surface engineering with ammonium niobium oxalate: A multifunctional strategy to enhance electrochemical performance and thermal stability of Ni-rich cathode materials at 4.5 V cutoff potential, *Electrochim. Acta*, 2022, **403**, 139636.

57 Y. Morino and S. Kanada, Degradation analysis by X-ray absorption spectroscopy for $LiNbO_3$ coating of sulfide-based all-solid-state battery cathode, *ACS Appl. Mater. Interfaces*, 2023, **15**, 2979–2984.

58 H. Yu, S. Wang, Y. Hu, G. He, L. Q. Bao, I. P. Parkin and H. Jiang, Lithium-conductive $LiNbO_3$ coated high-voltage $LiNi_{0.5}Co_{0.2}Mn_{0.3}O_2$ cathode with enhanced rate and cyclability, *Green Energy Environ.*, 2022, **7**, 266–274.

59 F. Xin, A. Goel, X. Chen, H. Zhou, J. Bai, S. Liu, F. Wang, G. Zhou and M. S. Whittingham, Electrochemical characterization and microstructure evolution of Ni-rich layered cathode materials by niobium coating/substitution, *Chem. Mater.*, 2022, **34**, 7858–7866.

60 X. Qu, H. Huang, T. Wan, L. Hu, Z. Yu, Y. Liu, A. Dou, Y. Zhou, M. Su, X. Peng, H.-H. Wu, T. Wu and D. Chu, An integrated surface coating strategy to enhance the electrochemical performance of nickel-rich layered cathodes, *Nano Energy*, 2022, **91**, 106665.

61 J. Li, Y. Zhu, B. Pang and P. Gao, Research on Nb doping–coating composite modification of $LiNiO_2$ cathode material for lithium-ion batteries, *J. Mater. Sci.*, 2022, **57**, 17722–17734.

62 E. Hassan, M. Amiriyan, D. Frisone, J. Dunham, R. Farahati and S. Farhad, Effects of coating on the electrochemical performance of a nickel-rich cathode active material, *Energies*, 2022, **15**, 4886.

63 M. H. Chiou, K. Borzutzki, J. H. Thienenkamp, M. Mohrhardt, K. L. Liu, V. Mereacre, J. R. Binder, H. Ehrenberg, M. Winter and G. Brunklaus, Durable fast-charging lithium metal batteries designed with cross-linked polymer electrolytes and niobate-coated cathode, *J. Power Sources*, 2022, **538**, 231528.

64 A. Zhu, J. Wu, B. Wang, J. Zhou, Y. Zhang, Y. Guo, K. Wu, H. Wu, Q. Wang and Y. Zhang, Harmonious dual-riveting interface induced from niobium oxides coating toward superior stability of Li-rich Mn-based cathode, *ACS Appl. Mater. Interfaces*, 2021, **13**, 61248–61257.

65 F. Xin, H. Zhou, X. Chen, M. Zuba, N. Chernova, G. Zhou and M. S. Whittingham, Li-Nb-O coating/substitution enhances the electrochemical performance of the $LiNi_{0.8}Mn_{0.1}Co_{0.1}O_2$ (NMC 811) cathode, *ACS Appl. Mater. Interfaces*, 2019, **11**, 34889–34894.

66 C. Lv, J. Yang, Y. Peng, X. Duan, J. Ma, Q. Li and T. Wang, 1D Nb-doped $LiNi_{1/3}Co_{1/3}Mn_{1/3}O_2$ nanostructures as excellent cathodes for Li-ion battery, *Electrochim. Acta*, 2019, **297**, 258–266.

67 A.-Y. Kim, F. Strauss, T. Bartsch, J. H. Teo, T. Hatsukade, A. Mazilkin, J. Janek, P. Hartmann and T. Brezesinski, Stabilizing effect of a hybrid surface coating on a Ni-rich NCM cathode material in all-solid-state batteries, *Chem. Mater.*, 2019, **31**, 9664–9672.

68 W. Pan, W. Peng, G. Yan, H. Guo, Z. Wang, X. Li, W. Gui, J. Wang and N. Chen, Suppressing the voltage decay and enhancing the electrochemical performance of $Li_{1.2}Mn_{0.54}Co_{0.13}Ni_{0.13}O_2$ by multifunctional Nb_2O_5 coating, *Energy Technol.*, 2018, **6**, 2139–2145.

69 G. Gabrielli, P. Axmann, T. Diemant, R. J. Behm and M. Wohlfahrt-Mehrens, Combining optimized particle morphology with a niobium-based coating for long cycling-life, high-voltage lithium-ion batteries, *ChemSusChem*, 2016, **9**, 1670–1679.

70 W. Sun, M. Xie, X. Shi and L. Zhang, Study of new phases grown on $LiNbO_3$ coated $LiCoO_2$ cathode material with an enhanced electrochemical performance, *Mater. Res. Bull.*, 2015, **61**, 287–291.

71 K. Takada, N. Ohta, L. Zhang, X. Xu, B. T. Hang, T. Ohnishi, M. Osada and T. Sasaki, Interfacial phenomena in solid-state lithium battery with sulfide solid electrolyte, *Solid State Ionics*, 2012, **225**, 594–597.

72 D. Kitsche, F. Strauss, Y. Tang, N. Bartnick, A.-Y. Kim, Y. Ma, C. Kübel, J. Janek and T. Brezesinski, A quasi-multinary composite coating on a nickel-rich NCM cathode material for all-solid-state batteries, *Batteries Supercaps*, 2022, **5**, e202100397.

73 S. Payandeh, F. Strauss, A. Mazilkin, A. Kondrakov and T. Brezesinski, Tailoring the $LiNbO_3$ coating of Ni-rich cathode materials for stable and high-performance all-solid-state batteries, *Nano Res. Energy*, 2022, **1**, e9120016.

74 Y. J. Kim, R. Rajagopal, S. Kang and K. S. Ryu, Novel dry deposition of $LiNbO_3$ or Li_2ZrO_3 on $LiNi_{0.6}Co_{0.2}Mn_{0.2}O_2$ for high performance all-solid-state lithium batteries, *Chem. Eng. J.*, 2020, **386**, 123975.

75 J. Wang, K. Wu, C. Xu, X. Hu and L. Qiu, $LiNbO_3$-coated $Li_{1.2}Mn_{0.54}Ni_{0.13}Co_{0.13}O_2$ as a cathode material with enhanced electrochemical performances for lithium-ion batteries, *J. Mater. Sci.: Mater. Electron.*, 2021, **32**, 28223–28233.

76 W. Zhang, L. Xiao, J. Zheng, Y. Zhong, B. Shi, H. Chen and H. Fu, Effect of Nb_2O_5 nanocoating on the thermal stability and electrochemical performance of $LiNi_{0.6}Co_{0.2}Mn_{0.2}O_2$ cathode materials for lithium ion batteries, *J. Alloys Compd.*, 2021, **880**, 160415.

77 L. Zhang, L. Xiao, J. Zheng, H. Wang, H. Chen and Y. Zhu, Effect of Nb^{5+} doping and $LiNbO_3$ coating on the structure and surface of a $LiNi_{0.8}Mn_{0.2}O_2$ cathode material for lithium-ion batteries, *J. Electrochem. Soc.*, 2021, **168**, 110528.

78 S. Liu, X. Chen, J. Zhao, J. Su, C. Zhang, T. Huang, J. Wu and A. Yu, Uncovering the role of Nb modification in improving the structure stability and electrochemical performance of $LiNi_{0.6}Co_{0.2}Mn_{0.2}O_2$ cathode charged at higher voltage of 4.5 V, *J. Power Sources*, 2018, **374**, 149–157.

79 T. Teng, L. Xiao, J. Zheng, D. Wen, H. Chen and Y. Zhu, High-Ni layered $LiNi_{0.83}Co_{0.11}Mn_{0.06}O_2$ modified by Nb for Li-ion batteries, *Ceram. Int.*, 2022, **48**, 8680–8688.

80 J. Liang, S. Hwang, S. Li, J. Luo, Y. Sun, Y. Zhao, Q. Sun, W. Li, M. Li, M. N. Banis, X. Li, R. Li, L. Zhang, S. Zhao, S. Lu, H. Huang, D. Su and X. Sun, Stabilizing and understanding the interface between nickel-rich cathode and PEO-based electrolyte by lithium niobium oxide coating for high-performance all-solid-state batteries, *Nano Energy*, 2020, **78**, 105107.

81 X. Liu, J. Shi, B. Zheng, Z. Chen, Y. Su, M. Zhang, C. Xie, M. Su and Y. Yang, Constructing a high-energy and durable single-crystal NCM811 cathode for all-solid-state batteries by a surface engineering strategy, *ACS Appl. Mater. Interfaces*, 2021, **13**, 41669–41679.

82 F. Walther, F. Strauss, X. Wu, B. Mogwitz, J. Hertle, J. Sann, M. Rohnke, T. Brezesinski and J. Janek, The working principle of a $Li_2CO_3/LiNbO_3$ coating on NCM for thiophosphate-based all-solid-state batteries, *Chem. Mater.*, 2021, **33**, 2110–2125.

83 F. Strauss, S. Payandeh, A. Kondrakov and T. Brezesinski, On the role of surface carbonate species in determining the cycling performance of all-solid-state batteries, *Mater. Futures*, 2022, **1**, 023501.

84 A.-Y. Kim, F. Strauss, T. Bartsch, J. H. Teo, J. Janek and T. Brezesinski, Effect of surface carbonates on the cyclability of $LiNbO_3$-coated NCM622 in all-solid-state batteries with lithium thiophosphate electrolytes, *Sci. Rep.*, 2021, **11**, 5367.

85 M. Nete, W. Purcell, E. Snyders and J. T. Nel, Alternative dissolution methods for analysis of niobium containing samples, *S. Afr. J. Chem.*, 2010, **63**, 130–134.

86 W. van den Bergh, H. N. Lokupitiya, N. A. Vest, B. Reid, S. Guldin and M. Stefik, Nanostructure dependence of T-Nb_2O_5 intercalation pseudocapacitance probed using tunable isomorphic architectures, *Adv. Funct. Mater.*, 2021, **31**, 2007826.

87 J. S. Lee and Y. J. Park, Comparison of $LiTaO_3$ and $LiNbO_3$ surface layers prepared by post- and precursor-based coating methods for Ni-rich cathodes of all-solid-state batteries, *ACS Appl. Mater. Interfaces*, 2021, **13**, 38333–38345.

88 X. Li, L. Jin, D. Song, H. Zhang, X. Shi, Z. Wang, L. Zhang and L. Zhu, $LiNbO_3$-coated $LiNi_{0.8}Co_{0.1}Mn_{0.1}O_2$ cathode with high discharge capacity and rate performance for all-solid-state lithium battery, *J. Energy Chem.*, 2020, **40**, 39–45.

89 L. Peng, H. Ren, J. Zhang, S. Chen, C. Yu, X. Miao, Z. Zhang, Z. He, M. Yu, L. Zhang, S. Cheng and J. Xie, $LiNbO_3$-coated $LiNi_{0.7}Co_{0.1}Mn_{0.2}O_2$ and chlorine-rich argyrodite enabling high-performance solid-state batteries under different temperatures, *Energy Storage Mater.*, 2021, **43**, 53–61.

90 F. Xin, H. Zhou, J. Bai, F. Wang and M. S. Whittingham, Conditioning the surface and bulk of high-nickel cathodes with a Nb coating: An in situ X-ray study, *J. Phys. Chem. Lett.*, 2021, **12**, 7908–7913.

91 R. S. Negi, S. P. Culver, M. Wiche, S. Ahmed, K. Volz and M. T. Elm, Optimized atomic layer deposition of homogeneous, conductive Al_2O_3 coatings for high-nickel NCM containing ready-to-use electrodes, *Phys. Chem. Chem. Phys.*, 2021, **23**, 6725–6737.

92 X. Li, J. Liu, M. N. Banis, A. Lushington, R. Li, M. Cai and X. Sun, Atomic layer deposition of solid-state electrolyte coated cathode materials with superior high-voltage cycling behavior for lithium ion battery application, *Energy Environ. Sci.*, 2014, **7**, 768–778.

93 G. Lu, W. Peng, Y. Zhang, X. Wang, X. Shi, D. Song, H. Zhang and L. Zhang, Study on the formation, development and coating mechanism of new phases on interface in $LiNbO_3$-coated $LiCoO_2$, *Electrochim. Acta*, 2021, **368**, 137639.

94 H. G. Kim and Y. J. Park, Synergy effect of K doping and Nb oxide coating on $Li_{1.2}Ni_{0.13}Co_{0.13}Mn_{0.54}O_2$ cathodes, *J. Electrochem. Sci. Technol.*, 2021, **12**, 377–386.

95 L. B. McCusker, R. B. Von Dreele, D. E. Cox, D. Louër and P. Scardi, Rietveld refinement guidelines, *J. Appl. Crystallogr.*, 1999, **32**, 36–50.

96 R. Jung, R. Morasch, P. Karayaylali, K. Phillips, F. Maglia, C. Stinner, Y. Shao-Horn and H. A. Gasteiger, Effect of ambient storage on the degradation of Ni-rich positive electrode materials (NMC811) for Li-ion batteries, *J. Electrochem. Soc.*, 2018, **165**, A132–A141.

97 Y. Liu, R. Yang, X. Li, W. Yang, Y. Lin, G. Zhang and L. Wang, Nb_2O_5 coating to improve the cyclic stability and voltage decay of Li-rich cathode material for lithium-ion battery, *Molecules*, 2023, **28**, 3890.

98 N. Özer and C. M. Lampert, Electrochemical lithium insertion in sol-gel deposited $LiNbO_3$ films, *Sol. Energy Mater. Sol. Cells*, 1995, **39**, 367–375.

99 Y. Deng, C. Eames, J.-N. Chotard, F. Lalère, V. Seznec, S. Emge, O. Pecher, C. P. Grey, C. Masquelier and M. S. Islam, Structural and mechanistic insights into fast lithium-ion conduction in Li_4SiO_4–Li_3PO_4 solid electrolytes, *J. Am. Chem. Soc.*, 2015, **137**, 9136–9145.

100 Y. Li, X. Chen, A. Dolocan, Z. Cui, S. Xin, L. Xue, H. Xu, K. Park and J. B. Goodenough, Garnet electrolyte with an ultralow interfacial resistance for Li-metal batteries, *J. Am. Chem. Soc.*, 2018, **140**, 6448–6455.

101 L. Chen, K. S. Chen, X. Chen, G. Ramirez, Z. Huang, N. R. Geise, H. G. Steinrück, B. L. Fisher, R. Shahbazian-Yassar, M. F. Toney, M. C. Hersam and J. W. Elam, Novel ALD chemistry enabled low-temperature synthesis of lithium fluoride coatings for durable lithium anodes, *ACS Appl. Mater. Interfaces*, 2018, **10**, 26972–26981.

102 S. Breuer, V. Pregartner, S. Lunghammer and H. M. R. Wilkening, Dispersed solid conductors: fast interfacial Li-ion dynamics in nanostructured LiF and LiF γ-Al_2O_3 composites, *J. Phys. Chem. C*, 2019, **123**, 5222–5230.

103 L. Yang, H. Zhang, J. Chen, H. Chen and Z. Li, Electrical conductivity of Al-doped Li_2ZrO_3 ceramics for Li-ion conductor electrolytes, *Ceram. Int.*, 2021, **47**, 17950–17955.

104 J. Li, M. Zhang, D. Zhang, Y. Yan and Z. Li, An effective doping strategy to improve the cyclic stability and rate capability of Ni-rich $LiNi_{0.8}Co_{0.1}Mn_{0.1}O_2$ cathode, *Chem. Eng. J.*, 2020, **402**, 126195.

105 W. Yan, S. Yang, Y. Huang, Y. Yang and G. Yuan, A review on doping/coating of nickel-rich cathode materials for lithium-ion batteries, *J. Alloys Compd.*, 2020, **819**, 153048.

106 H. H. Sun, U.-H. Kim, J.-H. Park, S.-W. Park, D.-H. Seo, A. Heller, C. B. Mullins, C. S. Yoon and Y.-K. Sun,

Transition metal-doped Ni-rich layered cathode materials for durable Li-ion batteries, *Nat. Commun.*, 2021, **12**, 6552.

107 G.-T. Park, B. Namkoong, S.-B. Kim, J. Liu, C. S. Yoon and Y.-K. Sun, Introducing high-valence elements into cobalt-free layered cathodes for practical lithium-ion batteries, *Nat. Energy*, 2022, **7**, 946–954.

108 Y.-H. Chen, J. Zhang, Y. Li, Y.-F. Zhang, S.-P. Huang, W. Lin and W.-K. Chen, Effects of doping high-valence transition metal (V, Nb and Zr) ions on the structure and electrochemical performance of LIB cathode material $LiNi_{0.8}Co_{0.1}Mn_{0.1}O_2$, *Phys. Chem. Chem. Phys.*, 2021, **23**, 11528–11537.

109 M. F. Kasim, W. A. H. W. Azizan, K. A. Elong, N. Kamarudin, M. K. Yaakob and N. Badar, Enhancing the structural stability and capacity retention of Ni-rich $LiNi_{0.7}Co_{0.3}O_2$ cathode materials via Ti doping for rechargeable Li-ion batteries: Experimental and computational approaches, *J. Alloys Compd.*, 2021, **888**, 161559.

110 D. Shumei, T. Dan, L. Ping, L. Huiqin, W. Fenyan and H. Zhang, Research progress and prospect in element doping of lithium-rich layered oxides as cathode materials for lithium-ion batteries, *J. Solid State Electrochem.*, 2023, **27**, 1–23.

111 Y. R. Luo, *Comprehensive handbook of chemical bond energies*, CRC Press, 2007.

112 G.-X. Huang, R.-H. Wang, X.-Y. Lv, J. Su, Y.-F. Long, Z.-Z. Qin and Y.-X. Wen, Effect of niobium doping on structural stability and electrochemical properties of $LiNiO_2$ cathode for Li-ion batteries, *J. Electrochem. Soc.*, 2022, **169**, 040533.

113 Z. Cui, X. Li, X. Bai, X. Ren and X. Ou, A comprehensive review of foreign-ion doping and recent achievements for nickel-rich cathode materials, *Energy Storage Mater.*, 2023, **57**, 14–43.

114 D. Rathore, C. Geng, N. Zaker, I. Hamam, Y. Liu, P. Xiao, G. A. Botton, J. Dahn and C. Yang, Tungsten infused grain boundaries enabling universal performance enhancement of Co-free Ni-rich cathode materials, *J. Electrochem. Soc.*, 2021, **168**, 120514.

115 N.-Y. Park, S.-B. Kim, M.-C. Kim, S.-M. Han, D.-H. Kim, M.-S. Kim and Y.-K. Sun, Mechanism of doping with high-valence elements for developing Ni-rich cathode materials, *Adv. Energy Mater.*, 2023, **13**, 2301530.

116 Z. Li, C. Luo, C. Wang, G. Jiang, J. Chen, S. Zhong, Q. Zhang and D. Li, Effects of Nb substitution on structure and electrochemical properties of $LiNi_{0.7}Mn_{0.3}O_2$ cathode materials, *J. Solid State Electrochem.*, 2018, **22**, 2811–2820.

117 X. Li, H. Xin, Y. Liu, D. Li, X. Yuan and X. Qin, Effect of niobium doping on the microstructure and electrochemical properties of lithium-rich layered $Li[Li_{0.2}Ni_{0.2}Mn_{0.6}]O_2$ as cathode materials for lithium ion batteries, *RSC Adv.*, 2015, **5**, 45351–45358.

118 T. Li, X. Chang, Y. Xin, Y. Liu and H. Tian, Synergistic strategy using doping and polymeric coating enables high-performance high-nickel layered cathodes for lithium-ion batteries, *J. Phys. Chem. C*, 2023, **127**, 8448–8461.

119 F. Tian, Y. Zhang, Z. Liu, R. de Souza Monteiro, R. M. Ribas, P. Gao, Y. Zhu, H. Yu, L. Ben and X. Huang, Investigation of structure and cycling performance of Nb^{5+} doped high-nickel ternary cathode materials, *Solid State Ionics*, 2021, **359**, 115520.

120 J. Wang, Z. Yi, C. Liu, M. He, C. Miao, J. Li, G. Xu and W. Xiao, Revealing the effect of Nb^{5+} on the electrochemical performance of nickel-rich layered $LiNi_{0.83}Co_{0.11}Mn_{0.06}O_2$ oxide cathode for lithium-ion batteries, *J. Colloid Interface Sci.*, 2023, **635**, 295–304.

121 M. Chu, Z. Huang, T. Zhang, R. Wang, T. Shao, C. Wang, W. Zhu, L. He, J. Chen, W. Zhao and Y. Xiao, Enhancing the electrochemical performance and structural stability of Ni-rich layered cathode materials via dual-site doping, *ACS Appl. Mater. Interfaces*, 2021, **13**, 19950–19958.

122 S. Jamil, M. Fasehullah, B. Jabar, P. Liu, M. K. Aslam, Y. Zhang, S. Bao and M. Xu, Significantly fastened redox kinetics in single crystal layered oxide cathode by gradient doping, *Nano Energy*, 2022, **94**, 106961.

123 Z. Zhao, C. Li, Z. Wen, Z. Yang, S. Lu, X. Zhang, S. Chen, B. Wu, F. Wu and D. Mu, Cation mixing effect regulation by niobium for high voltage single-crystalline nickel-rich cathodes, *Chem. Eng. J.*, 2023, **461**, 142093.

124 C. Zhang, B. Wei, W. Jiang, M. Wang, W. Hu, C. Liang, T. Wang, L. Chen, R. Zhang, P. Wang and W. Wei, Insights into the enhanced structural and thermal stabilities of Nb-substituted lithium-rich layered oxide cathodes, *ACS Appl. Mater. Interfaces*, 2021, **13**, 45619–45629.

125 H. Qian, H. Ren, Y. Zhang, X. He, W. Li, J. Wang, J. Hu, H. Yang, H. M. K. Sari, Y. Chen and X. Li, Surface doping vs. bulk doping of cathode materials for lithium-ion batteries: A review, *Electrochem. Energy Rev.*, 2022, **5**, 2.

126 T. Yoshida, K. Hongo and R. Maezono, First-principles study of structural transition in $LiNiO_2$ and high throughput screening for long life battery, *J. Phys. Chem. C*, 2019, **123**, 14126–14131.

127 Y. Liu, X. Wen, R. K. Lake and J. Guo, First-principles study of the doping effect in half delithiated $LiNiO_2$ cathodes, *ACS Appl. Energy Mater.*, 2023, **6**, 2134–2139.

128 Q. Hao, F. Du, T. Xu, Q. Zhou, H. Cao, Z. Fan, C. Mei and J. Zheng, Evaluation of Nb-doping on performance of $LiNiO_2$ in wide temperature range, *J. Electroanal. Chem.*, 2022, **907**, 116034.

129 H. Wu, X. Zhou, C. Yang, D. Xu, Y.-H. Zhu, T. Zhou, S. Xin and Y. You, Concentration-gradient Nb-doping in a single-crystal $LiNi_{0.83}Co_{0.12}Mn_{0.05}O_2$ cathode for high-rate and long-cycle lithium-ion batteries, *ACS Appl. Mater. Interfaces*, 2023, **15**, 18828–18835.

130 Y.-R. Kim, Y.-W. Yoo, D.-Y. Hwang, T.-Y. Shim, C.-Y. Kang, H.-J. Park, H.-S. Kim and S.-H. Lee, Effect of niobium doping to enhance electrochemical performances of $LiNi_{0.8}Co_{0.1}Mn_{0.1}O_2$ cathode material, *Solid State Ionics*, 2023, **389**, 116108.

131 Y. Zhang, C. Cui, J. Liu, Y. Bei, Y. Li, Z. Song, Y. Feng, H. Xu, S. Tian, Y. Song and F. Li, An effective modification strategy enhancing the structure stability and electrochemical performance of $LiNi_{0.5}Co_{0.2}Mn_{0.3}O_2$ cathode material for lithium-ion batteries, *J. Alloys Compd.*, 2021, **887**, 161480.

132 Z. Luo, G. Hu, W. Wang, Z. Peng, Z. Fang, Y. Cao, J. Huang and K. Du, Enhancing structural stability and electrochemical properties of Co-less Ni-rich layer cathode materials by fluorine and niobium co doping, *ACS Appl. Energy Mater.*, 2022, **5**, 10927–10939.

133 H. He, J. Dong, D. Zhang and C. Chang, Effect of Nb doping on the behavior of NCA cathode: Enhanced electrochemical performances from improved lattice stability towards 4.5 V application, *Ceram. Int.*, 2020, **46**, 24564–24574.

134 Y. Lei, J. Ai, S. Yang, C. Lai and Q. Xu, Nb-doping in $LiNi_{0.8}Co_{0.1}Mn_{0.1}O_2$ cathode material: Effect on the cycling stability and voltage decay at high rates, *J. Taiwan Inst. Chem. Eng.*, 2019, **97**, 255–263.

135 H.-Y. Lee, B.-K. Wu and M.-Y. Chern, Study on the formation of zinc peroxide on zinc oxide with hydrogen peroxide treatment using X-ray photoelectron spectroscopy (XPS), *Electron. Mater. Lett.*, 2014, **10**, 51–55.

136 K. Wu, G. Jia, X. Shangguan, G. Yang, Z. Zhu, Z. Peng, Q. Zhuge, F. Li and X. Cui, Improved high rate performance and cycle stability for $LiNi_{0.8}Co_{0.2}O_2$ by doping of the high valence state ion Nb^{5+} into Li^+ sites, *J. Alloys Compd.*, 2018, **765**, 700–709.

137 S. Liu, Z. Liu, X. Shen, W. Li, Y. Gao, M. N. Banis, M. Li, K. Chen, L. Zhu, R. Yu, Z. Wang, X. Sun, G. Lu, Q. Kong, X. Bai and L. Chen, Surface doping to enhance structural integrity and performance of Li-rich layered oxide, *Adv. Energy Mater.*, 2018, **8**, 1802105.

138 L. Li, E. C. Self, D. Darbar, L. Zou, I. Bhattacharya, D. Wang, J. Nanda and C. Wang, Hidden subsurface reconstruction and its atomic origins in layered oxide cathodes, *Nano Lett.*, 2020, **20**, 2756–2762.

139 J. Zhang, Z. Yang, R. Gao, L. Gu, Z. Hu and X. Liu, Suppressing the structure deterioration of Ni-rich $LiNi_{0.8}Co_{0.1}Mn_{0.1}O_2$ through atom-scale interfacial integration of self-forming hierarchical spinel layer with Ni gradient concentration, *ACS Appl. Mater. Interfaces*, 2017, **9**, 29794–29803.

140 E. D. Orlova, A. A. Savina, S. A. Abakumov, A. V. Morozov and A. M. Abakumov, Comprehensive study of Li^+/Ni^{2+} disorder in Ni-rich NMCs cathodes for Li-ion batteries, *Symmetry*, 2021, **13**, 1628.

141 H. Li, Z. Jian, P. Yang, J. Li, Y. Xing and S. Zhang, Niobium doping of $Li_{1.2}Mn_{0.54}Ni_{0.13}Co_{0.13}O_2$ cathode materials with enhanced structural stability and electrochemical performance, *Ceram. Int.*, 2020, **46**, 23773–23779.

142 X. Hu, H. Guo, W. Peng, Z. Wang, X. Li and Q. Hu, Effects of Nb doping on the performance of $0.5Li_2MnO_3\cdot 0.5LiNi_{1/3}Co_{1/3}Mn_{1/3}O_2$ cathode material for lithium-ion batteries, *J. Electroanal. Chem.*, 2018, **822**, 57–65.

143 J. Langdon and A. Manthiram, A perspective on single-crystal layered oxide cathodes for lithium-ion batteries, *Energy Storage Mater.*, 2021, **37**, 143–160.

144 W. van den Bergh, L. Karger, S. Murugan, J. Janek, A. Kondrakov and T. Brezesinski, Single crystal layered oxide cathodes: The relationship between particle size, rate capability, and stability, *ChemElectroChem*, 2023, **10**, e202300165.

145 B. Zhang, L. Cheng, P. Deng, Z. Xiao, L. Ming, Y. Zhao, B. Xu, J. Zhang, B. Wu and X. Ou, Effects of transition metal doping on electrochemical properties of single-crystalline $LiNi_{0.7}Co_{0.1}Mn_{0.2}O_2$ cathode materials for lithium-ion batteries, *J. Alloys Compd.*, 2021, **872**, 159619.

146 V. V. Atuchin, I. E. Kalabin, V. G. Kesler and N. V. Pervukhina, Nb 3d and O 1s core levels and chemical bonding in niobates, *J. Electron Spectrosc. Relat. Phenom.*, 2005, **142**, 129–134.

147 D. Norman, X-ray absorption spectroscopy (EXAFS and XANES) at surfaces, *J. Phys. C: Solid State Phys.*, 1986, **19**, 3273–3311.

148 B. H. Toby and T. Egami, Accuracy of pair distribution function analysis applied to crystalline and non-crystalline materials, *Acta Crystallogr., Sect. A: Found. Crystallogr.*, 1992, **48**, 336–346.

149 P. Kurzhals, F. Riewald, M. Bianchini, H. Sommer, H. A. Gasteiger and J. Janek, The $LiNiO_2$ cathode active material: A comprehensive study of calcination conditions and their correlation with physicochemical properties. Part I. Structural chemistry, *J. Electrochem. Soc.*, 2021, **168**, 110518.

150 D. Goonetilleke, B. Schwarz, H. Li, F. Fauth, E. Suard, S. Mangold, S. Indris, T. Brezesinski, M. Bianchini and D. Weber, Stoichiometry matters: Correlation between antisite defects, microstructure and magnetic behavior in the cathode material $Li_{1-z}Ni_{1+z}O_2$, *J. Mater. Chem. A*, 2023, **11**, 13468–13482.

151 A. Chakraborty, S. Kunnikuruvan, S. Kumar, B. Markovsky, D. Aurbach, M. Dixit and D. T. Major, Layered cathode materials for lithium-ion batteries: Review of computational studies on $LiNi_{1-x-y}Co_xMn_yO_2$ and $LiNi_{1-x-y}Co_xAl_yO_2$, *Chem. Mater.*, 2020, **32**, 915–952.

152 Y. Levartovsky, A. Chakraborty, S. Kunnikuruvan, S. Maiti, J. Grinblat, M. Talianker, D. T. Major and D. Aurbach, Enhancement of structural, electrochemical, and thermal properties of high-energy density Ni-rich $LiNi_{0.85}Co_{0.1}Mn_{0.05}O_2$ cathode materials for Li-ion batteries by niobium doping, *ACS Appl. Mater. Interfaces*, 2021, **13**, 34145–34156.

153 S. Ober, A. Mesnier and A. Manthiram, Surface stabilization of cobalt-free $LiNiO_2$ with niobium for lithium-ion batteries, *ACS Appl. Mater. Interfaces*, 2023, **15**, 1442–1451.

154 F. Strauss, D. Kitsche, Y. Ma, J. H. Teo, D. Goonetilleke, J. Janek, M. Bianchini and T. Brezesinski, Operando characterization techniques for all-solid-state lithium-ion batteries, *Adv. Energy Sustainability Res.*, 2021, **2**, 2100004.